Aquaculture drastically increases methane production by favoring acetoclastic rather than hydrogenotrophic methanogenesis in shrimp pond sediments

Ji Tan, Eric Lichtfouse, Min Luo, Yuxiu Liu, Fengfeng Tan, Changwei Zhang, Xin Chen, Jiafang Huang, Leilei Xiao

Aquaculture 563 (2023) 738999

https://doi.org/10.1016/j.aquaculture.2022.738999

Aquaculture drastically increases methane production by favoring acetoclastic rather than hydrogenotrophic methanogenesis in shrimp pond sediments

Ji Tan [a,b,c,d], Eric Lichtfouse [e], Min Luo [b,d,*], Yuxiu Liu [a,b,c], Fengfeng Tan [a,b,c], Changwei Zhang [a,b,d], Xin Chen [a,b,d], Jiafang Huang [a,b,c], Leilei Xiao [f,**]

[a] Key Laboratory of Humid Subtropical Eco-Geographical Process, Ministry of Education, Fujian Normal University, Fuzhou 350007, China
[b] Research Center of Geography and Ecological Environment, Fuzhou University, Fuzhou 350116, China
[c] College of Geography science, Fujian Normal University, Fuzhou 35008, China
[d] College of Environment and Safety Engineering, Fuzhou University, Fuzhou 350116, China
[e] Aix-Marseille Univ, CNRS, IRD, INRAE, CEREGE, Avenue Louis Philibert, Aixen Provence 13100, France
[f] CAS Key Laboratory of Coastal Environmental Processes and Ecological Remediation, Yantai Institute of Coastal Zone Research, Chinese Academy of Sciences, Yantai 264003, China

ARTICLE INFO

Keywords:
Methane
Coastal aquaculture pond
Isotopic fractionation factors
Acetoclastic methanogenesis
Hydrogenotrophic methanogenesis
Methanogenic community structure

ABSTRACT

Emissions of methane (CH_4), a major greenhouse gas, should be cut by at least 30% by 2030 according to the last Conference of the Parties, CoP26. Aquaculture pond is a major CH_4 emitter, yet the microbial mechanisms ruling methanogenesis by degradation of organic matter in sediments remain unclear. In particular, the respective roles of hydrogenotrophic and acetoclastic methanogenesis, and the impact of aquaculture farming practices are unknown. We studied methanogenesis in the surface sediments from a freshwater and an oligohaline pond before, during, and after shrimp farming. Hydrogenotrophic and acetoclastic contributions were distinguished by acetoclastic inhibition with methylfluoride (CH_3F), and by ^{13}C-analysis of CO_2 and CH_4. We also monitored the methanogenic community structure, dissolved organic carbon (DOC) levels, carbon to nitrogen (C/N) ratios, and humification indices derived from Fourier transform infrared spectroscopy. The results reveal that aquaculture farming practices increased methanogenesis rates, and these increases were explained by higher levels of DOC and lower C/N ratios during farming. Of the total methane produced, 51%–78% was by hydrogenotrophic methanogenesis. However, the total methane contribution from acetoclastic methanogenesis increased from approximately 22% before farming to approximately 45% during and after farming, with a decreasing isotope fractionation factor α_c and an increasing relative abundance of *Methanosaeta* acetoclastic methanogen. All humification indices decreased during and after farming compared to before farming due to the input of polysaccharide-rich aquafeed. The close relationship between the humification indices and methanogenesis pathways indicates that the changes in sediment substrate quality drove the variation in the methanogenesis pathways. Increases in salinity decreased the methanogenesis rates but did not change the methanogenesis pathways. Overall, our findings reveal that aquaculture farming practices increase methanogenesis rates and favor acetoclastic over hydrogenotrophic methanogenesis, and that adjusting shrimp diets, increasing salinity, and removing residual aquafeed could reduce methanogenesis.

1. Introduction

Methane, a major greenhouse gas, has a sustained global warming potential of 45 times higher than CO_2 over 100 years (Neubauer and Megonigal, 2015). Methane concentrations increased by approximately 156% from 1750 to 2019, with levels of CH_4 reaching a value of 1866.3

* Correspondence to: M. Luo, College of Environment and Safety Engineering, Fuzhou University, Wulongjiang North Avenue Street #2, Minhou County, Fuzhou 350116, China.
** Correspondence to: L. Xiao, CAS Key Laboratory of Coastal Environmental Processes and Ecological Remediation, Yantai Institute of Coastal Zone Research, Chinese Academy of Sciences, Yantai 264003, China.
E-mail addresses: luomin@fzu.edu.cn (M. Luo), llxiao@yic.ac.cn (L. Xiao).

± 3.3 ppb in 2019 (IPCC, 2021). Emissions of CH_4 should be cut by at least 30% by 2030 according to the last Conference of the Parties, CoP26 (European Union, 2021). Aquatic ecosystems (including lakes, reservoirs, and rivers) contributed 32%–58% of earth's total natural CH_4 emissions (Saunois et al., 2020). Small but numerous aquaculture ponds are essential components of aquatic ecosystems (Naylor et al., 2021). Coastal aquaculture ponds account for 50% of the global aquaculture ponds and are expected to increase 1.3-fold from 2010 to 2050 (Waite et al., 2014). Although coastal aquaculture ponds have been recently recognized as major anthropogenic sources of CH_4 (Cui et al., 2016; Song and Liu, 2015; Yang et al., 2018; Yang et al., 2020; Yuan et al., 2019), the underlying mechanisms of methanogenesis are unclear.

Methane is produced at the terminal step of organic matter degradation (Conrad et al., 2010b). Organic matter is fermented to acetate, H_2, and CO_2, which are converted to CH_4 by methanogenic archaea (Conrad et al., 2010b; Xiao et al., 2020a). Acetoclastic and hydrogenotrophic are the two main pathways of methanogenesis in low-salinity aquatic systems (Conrad, 2005):

- Acetoclastic methanogenesis: $CH_3COOH \rightarrow CH_4 + CO_2$.
- Hydrogenotrophic methanogenesis: $4H_2 + CO_2 \rightarrow CH_4 + H_2O$.

Indeed, methanogens have preference for either H_2 or acetate substrates (Conrad et al., 2007; Etminan et al., 2016). For instance, *Methanoregula*, *Methanobacterium*, *Methanospirillum*, *Methanolinea*, and *Methanogenium* prefer H_2, whereas *Methanosaeta* prefer acetate (Liu and Whitman, 2008; Sakai et al., 2008). Some methanogens, for example, *Methanosarcina*, are mixotrophs, which can use both H_2 and acetate substrates (Penger et al., 2012). Nevertheless, two strategies allow us to experimentally distinguish the relative importance of two pathways: the addition of methylfluoride (CH_3F) to inhibit acetoclastic methanogenesis, and measuring ^{13}C isotope ratios of CO_2 and CH_4 (Conrad et al., 2020; Xiao et al., 2020b). The isotope fractionation is valid because hydrogenotrophic methanogens produces lighter methane with the $\delta^{13}CH_4$ ranging from −110‰ to −60‰, whereas acetoclastic methanogenesis produces heavier methane with the $\delta^{13}CH_4$ ranging from −70‰ to −30‰ (Conrad, 2005; Hodgkins et al., 2014).

Methanogenesis is theoretically governed by stoichiometric equivalence, i.e., 67% of the CH_4 is produced by acetoclastic methanogenesis, whereas 33% comes from the reduction of CO_2 with H_2 (Conrad, 1999). Nonetheless, in sediments of lakes (Mandic-Mulec et al., 2012), rivers (Mach et al., 2015; Qin et al., 2020), coves (King et al., 1983), paddies (Ji et al., 2018), peatlands (Hines et al., 2008; Kotsyurbenko et al., 2004; Krohn et al., 2017), and wetlands (Li et al., 2018; Xiao et al., 2019), the contribution of acetoclastic methanogenesis to the total methanogenesis varied from 0.5% to 99%. The contribution of each methanogenesis pathway depends on the pH (Ye et al., 2012), temperature (Chen and Chang, 2020), and more importantly, organic matter quantity and quality of the sediments (Corbett et al., 2015; Liu et al., 2012; Hofmann et al., 2016).

Farming practices could significantly alter methanogenesis rates in aquaculture pond systems. Indeed, large temporal variations in CH_4 emission flux across farming periods have been reported in various aquaculture pond systems (Ma et al., 2018; Song and Liu, 2015; Tong et al., 2021; Yang et al., 2019). Yet, little is known about how farming practices affect methanogenesis pathways in aquaculture pond systems. Nevertheless, several studies have reported that farming practices can modify the organic matter quality and quantity of sediments (Ali et al., 2021; Mulat et al., 2016; Pusceddu et al., 2011; Sabu et al., 2022; Wu and Song, 2021). For instance, in grass carp (*Ctenopharyngodon idella*) aquaculture ponds, carp feeding increased sediment dissolved organic carbon (DOC) concentrations by 2–5 times (Chen et al., 2015). Furthermore, in a *Labeo victorianus* pond, the total nitrogen contents from the pre-farming to post-farming periods increased from 1.58 to 1.84 mg g^{-1} (Magondu et al., 2013). Additionally, in a shrimp (*Litopenaeus stylirostris*) pond in New Caledonia, from the initial stage to the last stage of shrimp farming, the protein content increased from 3.8 to 5.9 mg g^{-1}, while the lipid content increased from 1.2 to 3.0 mg g^{-1} (Pusceddu et al., 2011). Such changes in the substrate quality and quantity of the sediments could affect the accumulation of H_2, CO_2, and acetate and thus, change the methanogenesis pathway (Berberich et al., 2020; Holmes et al., 2015). Consequently, it is reasonable to expect that methanogenesis rates and pathways differ across aquaculture stages, although there is currently a paucity of actual field data to demonstrate this hypothesis.

Salinity is another important environmental driver affecting the rates of methanogenesis. In numerous coastal wetland studies, methanogenesis was shown to decrease with salinity (Luo et al., 2019a; Neubauer et al., 2013; Chambers et al., 2013), and similar results were also reported in aquaculture pond systems. For instance, a prior study suggested that the CH_4 emission fluxes in the ponds with a salinity of 1.9‰–3.4‰ were approximately 10 times higher than those of the ponds with a salinity of 6.1‰–15.1‰ (Yang et al., 2018). In algae-shellfish mariculture ponds, net CH_4 exchange was also found to decrease with increasing salinity (Zhang et al., 2022). Furthermore, studies have reported that methanogenic community composition varies significantly with changing salinity since different methanogen taxa have different salinity tolerances (Chen et al., 2020; Liu et al., 2016). For instance, *Methanomethylovorans* only can live in sediments with salinity below 1.7‰ (Bräuer et al., 2011), while *Methanomassiliicoccus* and *Methanospirillum* can tolerate salinities of 10‰–15‰ (Dridi et al., 2012). A study in the lake sediments of the Tibetan Plateau has even suggested that the distribution patterns of hydrogenotrophic and acetotrophic methanogens are related to changes in salinity (Liu et al., 2016). Therefore, variation in salinity between ponds may affect methanogenesis pathways in coastal aquaculture pond systems. A more comprehensive understanding of the responses of methanogenesis pathways to salinity may help us to better understand methanogenesis mechanisms in aquaculture systems.

To bridge these knowledge gaps, we investigated methanogenesis before, during, and after farming, in a freshwater and an oligohaline pond in the Min River Estuary, East China Sea. To isolate the effects of aquaculture farming practices and salinity, the selected ponds were similar in terms of size, sediment texture, bulk density, and adopted the consistent aquiculture management practices for all three aquaculture farming stages (Table 1 and Fig. 1). We monitored the methanogenesis and distinguished the contribution of acetoclastic versus hydrogenotrophic methanogenesis by CH_3F addition, measuring $\delta^{13}CO_2$ and $\delta^{13}CH_4$, and investigating the methanogenic community structure. The specific goal of this study was to: (i) clarify how aquaculture farming practices affect rates and pathways of methanogenesis across three aquaculture farming stages; and (ii) identify whether methanogenesis metabolism differs between freshwater and oligohaline ponds. We hypothesized that (i) aquaculture farming practices increase the rates of methanogenesis and contribute to acetoclastic methanogenesis because of the introduction of polysaccharide-rich aquafeeds; (ii) oligohaline ponds have lower methanogenesis rates than freshwater ponds because of the salt stress.

Table 1
Location, pond size, sediment texture, bulk density, and maximum water depth (means ± standard deviation, n = 3 biological replicates) of the freshwater and oligohaline ponds in the Min River Estuary, southeast China.

	Ponds	
	Freshwater	Oligohaline
Latitude	26°03′03″N	26°01′32″N
Longitude	119°33′33″E	119°38′04″E
Pond size (hm^2)	1.644	1.615
Sand (%)	15.2 ± 1.7	15.2 ± 2.8
Slit (%)	67.9 ± 2.2	66.9 ± 2.8
Clay (%)	16.9 ± 1.3	17.3 ± 0.9
Bulk density (g cm^{-3})	1.11 ± 0.23	1.20 ± 0.25
Maximum water depth (m)	1.51 ± 0.20	1.58 ± 0.17

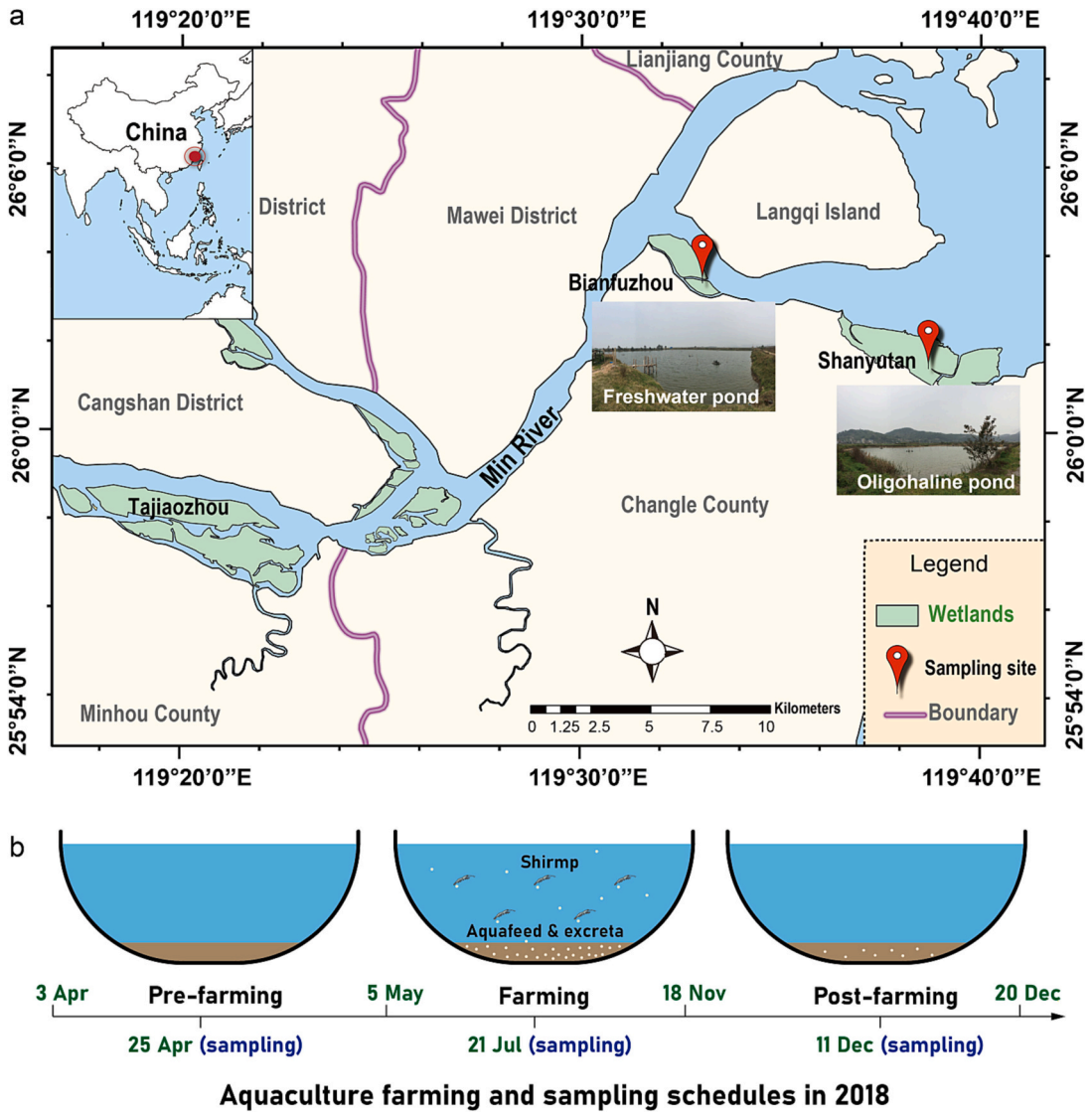

Fig. 1. (a) Location of the freshwater and the oligohaline ponds in the Min River Estuary, southeast China. (b) Aquaculture farming and sampling schedules across the aquaculture farming stages in 2018.

2. Materials and methods

2.1. Location and sampling strategy

The study was conducted in monoculture ponds of white shrimp, *Litopenaeus vannamei*, in the Min River Estuary, southeast China (26°00′N–26°05′N, 119°30′E–119°41′E). White shrimp accounted for 53% of total global crustacean production in 2016, and is one of the most important commercial species in the local coastal aquaculture industry (FAO, 2018). The climate in the study area is subtropical marine monsoon with an annual average temperature of 19.6 °C and an annual average precipitation of 1350 mm (www.weather.com.cn). We selected a freshwater pond, with salinity of 0.3‰–0.4‰, and an oligohaline pond, with salinity of 3.3‰–3.8‰, along the Min River Estuary (Fig. 1a). *L. vannamei* is a euryhaline shrimp species that could grow well in both ponds. The ponds were similar in size, maximum water depth, sediment texture, and bulk density (Table 1). Both ponds were converted from *Cyperus malaccensis* wetlands 7–9 years ago.

Aquaculture farming management was consistent for the two ponds during the experimental period from April to December 2018 (Fig. 1b). Specifically, during the pre-farming stage (April 3–May 4, 2018), the residual sludge from the previous harvest was removed mechanically and water from nearby estuaries was introduced into the ponds. There was no water exchange during the farming and post-farming periods. Also, the maximum water depth of the two ponds ranged from 1.51 ± 0.20 m to 1.58 ± 0.17 m (Table 1). During the farming stage (May 5–November 17, 2018), the shrimp larvae were released into the ponds on May 5. The aquafeed was commercial aquatic feed pellets (including crude protein 31.1%, crude fat 6.8%, moisture 8.7%, ash 5.3%, and fiber 1.1%) and was added to the ponds twice a day. The feeding rates were 10–15, 40–50, and 30–40 kg ha^{-1} d^{-1} during the growth periods of the larvae, juveniles, and adults, respectively. On average, a total of ~3.0 t of aquafeed was added to each pond during the farming period. Then, the shrimps were harvested from November 12 to November 17, 2018. During the post-farming stage (November 18–December 20, 2018), the aquaculture wastewater remained in the ponds, and no more artificial disturbance occurred.

2.2. Sediment and porewater collection

In 2018, sediment sampling was conducted at the pre-farming stage (April 25), farming stage (July 21), and post-farming stage (December 11) in both shrimp ponds (Fig. 1b). During sediment sampling, PVC tubes (length: 10 cm; inner diameter: 10 cm) were randomly inserted

into the pond sediments. Each pond had three biological replicates within one stage. The sampling depth was 0–5 cm as this layer was the most impacted by aquaculture farming practices (Suárez-Abelenda et al., 2014; Tho et al., 2011). Sediments were bubbled using nitrogen (N_2) and closed with silicone gaskets on both ends before being stored on ice and being transferred to the laboratory. Sediment samples were pooled, homogenized, and sieved (2 mm mesh size) in an anaerobic glove bag from AtmosBag, Sigma-Aldrich. Sediment subsamples for the molecular genetic analyses were immediately snap frozen in liquid nitrogen and stored at − 80 °C. The porewater samples for determining sulfate (SO_4^{2-}), DOC, ammonia (NH_4^+), and nitrate (NO_3^-) concentrations were extracted by centrifuging the sediment subsamples for 6 min at 4000 rpm and were filtered through 0.45-μm pore size membrane filters. Sediment and porewater subsamples were stored at 4 °C and the analyses were completed within 7 days.

2.3. Sediment and porewater properties analyses

Sediment total organic carbon (TOC) and total nitrogen (TN) were measured using a CN-elemental analyzer with detection limits of 0.02 mg g^{-1} (Vario MAX CN, Germany). Prior to performing the TOC measurements, sediments were leached with 10% HCl to remove inorganic carbon, washed with distilled water at pH 7, then dried at room temperature (Hou et al., 2013). The C/N ratio refers to the TOC versus the TN. Sediment temperature was measured by using a Thermo Fisher Scientific Temp 10 Series thermometer, with a detection accuracy of 0.1 °C. Sediment pH was measured using a Thermo Fisher Scientific pH 450 pH meter, with a detection accuracy of 0.1. Porewater salinity was measured using a salinity meter (SALT 6+, Eutech instruments, Thermo Fisher Scientific), with a detection accuracy of 0.1‰. The DOC concentrations were analyzed using a TOC-VCPH analyzer from Shimadzu, with a detection limit of 2 μmol L^{-1}. Porewater SO_4^{2-} concentrations were analyzed in an ICS-2000 Dionex ion chromatograph (Thermo Fisher Scientific) with a detection limit of 2 μmol L^{-1}. Porewater NH_4^+ and NO_3^- concentrations were analyzed by the sodium hypobromite and copper-cadmium reduction method, respectively (Zhang et al., 2014). Porewater NH_4^+ and NO_3^- concentrations were determined using a San++ continuous flow analyzer (Skalar Analytical) with detection limits of 2 μmol L^{-1} and 1 μmol L^{-1}, respectively.

2.4. Fourier-transform infrared spectroscopy

The relative abundance of the different sediment C compound classes in the sediment powders were determined by attenuated total reflectance Fourier-transform infrared spectroscopy (ATR-FTIR) using a Nicolet iS10 instrument (Thermo Fisher Scientific). The spectra were acquired by averaging 32 scans at 4-cm^{-1} resolution over 800–3500 cm^{-1}. The spectra were corrected for the ATR to allow for differences in the depth of the beam penetration at different wavelengths, and then baseline was corrected using the instrument software. The humification indices were calculated using the ratio of the absorbance of aliphatics, aromatic esters, lignin and aromatics with the polysaccharides following the methodology described by Beer et al. (2008).

2.5. Incubation experiments

The incubation procedure followed the methods of Conrad et al. (2007). Approximately 20 g sediment subsamples were slurried and deoxygenated with in-situ filtered pondwater (1:2, *w*/w) in a nitrogen atmosphere, transferred into 175 mL sterile serum bottles, flushed with N_2, closed with butyl rubber stoppers, and then incubated at room temperature (20–23 °C) in the dark. Methyl fluoride (CH_3F) was added to the headspace of half of the bottles at 2% (vol/vol) of the bottle volume to inhibit acetoclastic methanogenesis. Gas samples were collected at 1– 7 days intervals, depending on the CO_2 and CH_4 production rates. Before sampling, the bottles were vigorous shaken, and the headspace pressure was measured using a pressure gauge (SSI technologies). Then, 0.5 mL of the headspace gas was injected into 20-mL airtight gas sampling bags that were pre-evacuated and filled with 10 mL helium gas, for the CO_2 and CH_4 analysis. After the gas was sampled, the bottles were backfilled with 0.5-mL N_2 to re-establish normal atmospheric pressure. The concentrations of the CO_2 and CH_4 were determined using a GC-2010 Shimadzu gas chromatography equipped with a packed Porapak Q column and a flame ionization detector. Prior to the chromatography, the CO_2 was converted to CH_4 by reduction with H_2 in a nickel reactor at 350 °C. The CO_2 and CH_4 detection limits were 10 ppm and 0.3 ppm, respectively.

2.6. Isotope analysis

After 60 days of incubation, 15 mL of the headspace gas was sampled then overpressure injected into 12 mL pre-evacuated exetainer sample vials for the $\delta^{13}C$ isotope analysis. The $\delta^{13}C$ isotope analysis was performed using a GasBench-PreCon trace gas system coupled to a Delta *V* Plus IRMS from Thermo Scientific. Gas samples (0.5 mL) were used to determine the isotopic composition of the released CO_2. Analyses of the $\delta^{13}CH_4$ used a Precon-Gas Bench-Isotope Ratio Mass Spectrometer (Precon-GB-IRMS) with gas samples (10 mL) injected into the Precon with a helium carrier gas. The $^{13}C/^{12}C$ isotope ratios were expressed as $\delta^{13}C$ relative to the international standards of Vienna Pee Dee Belemnite (V-PDB), where $\delta^{13}C = (R_{sample} / R_{standard} - 1) \times 1000$, and R_{sample} and $R_{standard}$ are the $^{13}C/^{12}C$ ratios in the sample and the PDB standard, respectively. Since the $\delta^{13}CH_4$ also depends on $\delta^{13}CO_2$, the isotope fractionation factor, α_c: $(\delta^{13}CO_2 + 10^3) / (\delta^{13}CH_4 + 10^3)$ is calculated to distinguish the contributions of CH_4 and CO_2 (Whiticar, 1999).

2.7. Genetic analysis

DNA was extracted from 0.25 g of each sediment sample using the MOBIO Laboratories PowerSoil DNA Isolation Kit. Real-time quantitative polymerase chain reaction (qPCR) assays were used to assess the abundance of methanogenic groups using the specific primers mlas-mod-F (5′-GGYGGTGTMGGDTTCACMCARTA-3′) and mcrA-rev-R (5′-CGTTCATBGCGTAGTTVG GRTAGT-3′) (Steinberg and Regan, 2008). The qPCR assays of the standards and samples were performed using the Thermo Fisher Scientific Applied Biosystems 7500 Real-Time PCR System. The reaction efficiencies for *mcrA* gene groups were 91.3%, with an r^2 above 0.99. The results were reported as the number of gene copies per gram of dry sediment.

High-throughput amplicon sequencing was performed using an Miseq PE300 sequencing platform (Illumina Inc., CA, USA). For amplicon sequencing, the *mcrA* gene fragments were amplified using the primer pair mlas-mod-F and mcrA-rev-R (Steinberg and Regan, 2008). The qualified reads were separated using the sample-specific barcode sequences and trimmed using Illumina Analysis Pipeline version 2.6. The datasets were analyzed using QIIME1.8.0 (http://qiime.org/; Caporaso et al., 2012). A total of 470,017 high-quality Illumina sequence reads were obtained for the *mcrA* genes. Rarefaction analysis was used to rarefy the operational taxonomic unit (OTU) tables to count to 26,444 reads for *mcrA* gene sequences. This was the lowest sequencing depth obtained from a sample, and was therefore used as the threshold for rarefaction calculations (Gotelli and Colwell, 2001). The sequences were assigned to OTUs by referencing with a subset of the SILVA 128 database for *mcrA* genes.

2.8. Data analysis

All analyses were conducted using R software (version 4.0.3; R Core Team, 2013). We applied modified Gompertz models to fit the CO_2 and CH_4 accumulation curves (Zwietering et al., 1990):

$$M_t = M_0 \cdot exp\left\{ -exp\left[\frac{R_{max} \cdot e}{M_o}(\lambda - t) + 1\right]\right\} \quad (1)$$

where M_t (μg g^{-1}) denotes the cumulative methanogenesis per gram of dry sediment; M_0 (μg g^{-1}) denotes the maximum methanogenesis per gram of dry sediment by the end of incubation; t (d) denotes the incubation time; R_{max} (μg g^{-1} d^{-1}) denotes the maximum methanogenesis rates per gram of dry sediment; λ (d) denotes the time lag. The fitting results were determined by r^2 with a significant level of $p < 0.05$. Model fitting used the '*nls*' function. The rates of CO_2 production, CH_4 production, and hydrogenotrophic methanogenesis were equal to the R_{max} that was derived from the accumulation curves of CO_2, CH_4, and CH_4 with an inhibitor, respectively. The rates of acetoclastic methanogenesis were calculated using the difference between CH_4 production rates and hydrogenotrophic methanogenesis rates.

The contribution of the CH_4 production rates to the total sum of the production rates of CH_4 and CO_2 (i.e., f_{CH4}) was calculated as follows:

$$f_{CH4} = CH_4 \text{ production rates}/(CH_4 + CO_2) \text{ production rates} \quad (2)$$

The contribution of acetoclastic methanogenesis to the total CH_4 production rates (i.e., $f_{acetoclastic}$) was calculated as follows:

$$f_{acetoclastic} = \text{Acetoclastic methanogenesis rates}/CH_4 \text{ production rates} \quad (3)$$

Two-way analysis of variance (ANOVA) was used to explore the primary and interactive effects of farming practices and the salinity on the sediment and porewater properties, CH_4 and CO_2 production rates, hydrogenotrophic and acetoclastic methanogenesis rates, f_{CH4}, $f_{acetoclastic}$, and the abundance of *mcrA* genes at a significance level of $p < 0.05$. Prior to performing ANOVA, all datasets were analyzed to identify whether they met the assumptions of homogeneity (the Brown and Forsythe test) and normality (the Shapiro-Wilk test) and data was log_{10}- or box-cox transformed if the transformation substantially improved the distribution. The ANOVA was calculated using the '*aov*' function. Multiple comparisons across the three aquaculture farming stages were calculated using one-way ANOVAs followed by a Tukey's HSD post hoc test. Pairwise comparisons between the freshwater and oligohaline ponds were performed using the paired-sample *t*-tests. Pearson correlations between the methanogenesis rates and environmental variables were calculated using the '*cor*' function with significance at $p < 0.05$. Linear regression models were used to examine the relationships between the humification indices and the $f_{acetoclastic}$ using the '*lm*' function with significance at $p < 0.05$. The beta diversity of the methanogenic community composition was visualized using Nonmetric Multidimensional scaling analyses (NMDS) with a weighted Bray-Curtis distance. Dissimilarity tests were performed by two-way PerMANOVA (permutational multivariate analysis of variance) based on the Bray-Curtis distance. The NMDS and PerMANOVA were calculated using the '*vegan*' package.

A hypothesized structural equation model was built (Fig. S2) to access the impact of aquaculture farming practices and salinity on rates and pathways of methanogenesis using '*lavaan*' package (Rosseel, 2012). After the initial model was evaluated, we went through a process of adding/removing pathways and variables. The goodness of fit was assessed based on a chi-squared (χ^2) test, the Comparative Fit Index, and the Akaike Information Criterion values.

3. Results

3.1. Sediment and porewater properties

Both the freshwater and oligohaline ponds possessed a higher sediment temperature (of approximately 30 °C) in the farming stage compared with the pre-farming stage (approximately 24 °C) and the post-farming stage (approximately 18 °C) ($p < 0.001$; Table 2). The sediment pH was 7.6–8.1 and did not significantly vary between the two ponds or with the farming stages ($p > 0.05$; Table 2). The freshwater pond samples had lower porewater salinity and sulfate concentrations than the oligohaline pond samples ($p < 0.001$; Table 2). The porewater salinity and sulfate concentrations were similar in all three farming stages in each pond ($p > 0.05$; Table 2). The TOC contents (range: 21.1–24.5 mg g^{-1}) were similar between the ponds and aquaculture farming stages ($p > 0.05$; Table 2). The C/N ratios (range: 8.8–11.3) and the DOC concentrations (range: 8.8–19.9 mmol L^{-1}) did not vary between the ponds ($p > 0.05$; Table 2). However, lower C/N ratios and higher DOC concentrations occurred in the farming and post-farming stages compared with the pre-farming stage ($p < 0.01$; Table 2). The porewater NH_4^+ concentrations ranged from 44.7 to 201.9 μmol L^{-1} (Table 2), while the porewater NO_3^- concentrations ranged from 1.0 to 2.8 μmol L^{-1} (Table 2). The porewater NH_4^+ and NO_3^- concentrations were higher in the farming and post-farming stages compared with the pre-farming stage ($p < 0.001$; Table 2).

Table 2
Sediment and porewater properties (means ± standard deviation, n = 3 biological replicates) across three aquaculture farming stages of the freshwater and oligohaline shrimp ponds in the Min River Estuary, southeast China.

	Ponds	Stages			Factor	Two-way ANOVA		
		Pre-farming	Farming	Post-farming		Stage	Pond	Interaction
Sediment temperature (°C)	Freshwater	23.6 ± 0.2B	30.4 ± 0.3A	18.2 ± 0.2C	***F***	**4628.839**	4.598	3.322
	Oligohaline	24.2 ± 0.2B	30.5 ± 0.2A	18.3 ± 0.3C	***P***	**<0.001**	>0.05	>0.05
pH	Freshwater	8.0 ± 0.3A	7.6 ± 0.1A	7.9 ± 0.2A	***F***	2.803	0.115	0.234
	Oligohaline	8.1 ± 0.4A	7.8 ± 0.2A	7.9 ± 0.2A	***P***	>0.05	>0.05	>0.05
Salinity (‰)	Freshwater	0.4 ± 0.1A**	0.3 ± 0.0A**	0.3 ± 0.0A**	***F***	1.696	**907.837**	2.130
	Oligohaline	3.3 ± 0.3A	3.5 ± 0.2A	3.8 ± 0.3A	***P***	0.225	**<0.001**	0.162
SO_4^{2-} (mmol L^{-1})	Freshwater	0.04 ± 0.01A**	0.03 ± 0.00A*	0.03 ± 0.01A**	***F***	0.542	**336.03**	0.308
	Oligohaline	0.42 ± 0.05A	0.38 ± 0.06A	0.41 ± 0.06A	***P***	0.595	**<0.001**	0.740
TOC (mg g^{-1})	Freshwater	22.0 ± 2.0A	22.7 ± 1.5A	23.8 ± 2.6A	***F***	1.514	0.004	0.646
	Oligohaline	21.1 ± 2.5A	24.5 ± 3.0A	23.1 ± 1.8A	***P***	>0.05	>0.05	>0.05
C/N ratio	Freshwater	11.3 ± 1.2A	9.0 ± 0.4B	9.9 ± 0.4B	***F***	**11.129**	1.456	0.176
	Oligohaline	10.6 ± 1.0A	8.8 ± 0.9B	9.4 ± 0.5B	***P***	**0.002**	>0.05	>0.05
DOC (mmol L^{-1})	Freshwater	8.8 ± 0.6C	17.8 ± 2.2A	14.0 ± 1.6B	***F***	**54.820**	4.016	0.192
	Oligohaline	9.7 ± 1.3C	19.9 ± 1.4A	15.6 ± 2.0B	***P***	**<0.001**	>0.05	>0.05
NH_4^+ (μmol L^{-1})	Freshwater	44.7 ± 9.2B	141.0 ± 16.5A	173.3 ± 12.6A	***F***	**174.876**	4.676	1.452
	Oligohaline	47.9 ± 10.9B	150.2 ± 17.4A	201.9 ± 12.2A	***P***	**<0.001**	>0.05	>0.05
NO_3^- (μmol L^{-1})	Freshwater	1.0 ± 0.2C	1.5 ± 0.3B	2.6 ± 0.2A	***F***	**48.180**	2.597	0.050
	Oligohaline	1.2 ± 0.2C	1.8 ± 0.4B	2.8 ± 0.4A	***P***	**<0.001**	>0.05	>0.05

Different uppercase letters indicate significant differences across all three farming stages.
Asterisks denote significant difference between the ponds within a single stage (*$p < 0.05$; **$p < 0.01$; ***$p < 0.001$).
Bold letters denote significant differences at $p < 0.05$.

3.2. Chemical composition of organic matter

The main compounds in the sediment organic matter in ponds are polysaccharides, lignin, and aromatics (aromatic esters and aliphatics) (Fig. S1). All samples possessed similar compounds, but we observed changes in their relative abundances across three farming stages. The humification indices decreased from 0.04 to 0.13 before shrimp farming commenced to 0.01–0.05 during farming and 0.02–0.07 after farming ($p < 0.001$; Table 3). The humification indices were not significantly different between the freshwater and oligohaline ponds ($p > 0.05$; Table 3).

3.3. Production of CH_4 and CO_2 during sediment incubation

Incubating the pond sediments induced a rapid increase in the cumulative CH_4 and CO_2 concentrations during the first 16 days, then plateaued until day 60 (Fig. 2). The addition of CH_3F (an inhibitor of acetoclastic methanogenesis) clearly inhibited the CH_4 production in both the freshwater and oligohaline sediments, while the CO_2 production was not significantly modified (Fig. 2). The CH_4 and CO_2 production curves fitted the modified Gompertz models with r^2 coefficients above 0.85 ($p < 0.001$) (Fig. 2 and Table S1).

Methanogenesis rates in the sediments ranged from 0.11 to 0.54 μg g^{-1} d^{-1}, and the CO_2 production rates ranged from 6.2 to 29.5 μg g^{-1} d^{-1}. Across the three aquaculture farming stages, the CH_4 and CO_2 production rates had higher levels in the farming and post-farming stages, when compared with the pre-farming stage ($p < 0.001$; Fig. 3a and b). The f_{CH4} was comparable in all three aquaculture farming stages ($p > 0.05$; Fig. 3c). The freshwater pond had relatively higher CH_4 production rates but lower CO_2 production rates compared with the oligohaline pond ($p < 0.01$; Fig. 3a and b), resulting in higher values of f_{CH4} in the freshwater pond than the oligohaline pond ($p < 0.001$; Fig. 3c).

The hydrogenotrophic methanogenesis rates ranged from 0.08 to 0.29 μg g^{-1} d^{-1}, and the acetoclastic methanogenesis rates ranged from 0.02 to 0.26 μg g^{-1} d^{-1} (Fig. 3d and e). Both the hydrogenotrophic and acetoclastic methanogenesis rates were higher in the farming and post-farming stages, compared with the rates in the pre-farming stage ($p < 0.01$; Fig. 3d and e). Moreover, the $f_{acetoclastic}$ were higher at the farming stages and post-farming stages than the pre-farming stages ($p < 0.001$; Fig. 3f). Both the hydrogenotrophic and acetoclastic methanogenesis rates were higher in the freshwater pond than the oligohaline pond ($p < 0.05$; Fig. 3d and e). However, the $f_{acetoclastic}$ did not vary between the freshwater and oligohaline ponds ($p > 0.05$; Fig. 3f).

3.4. Isotope analysis of CH_4 and CO_2

In the pond sediments, the $\delta^{13}CH_4$ ranged from −87‰ to −72‰, whereas the $\delta^{13}CO_2$ ranged from −21‰ to −18‰ (Fig. 4a and b). The $\delta^{13}CH_4$ and $\delta^{13}CO_2$ were not significantly different between the oligohaline and freshwater ponds ($p > 0.05$; Fig. 4a and b). The $\delta^{13}CH_4$ were lower prior to farming, compared with the farming and post-farming stages ($p < 0.001$; Fig. 4a). The isotopic fractionation factors (α_c) were lower in the farming and post-farming stages (1.055–1.062), compared with pre-farming stage ($p < 0.001$; 1.070–1.074) (Fig. 4c).

3.5. Methanogenic community abundance and composition

The abundance of *mcrA* gene in the sediments ranged from 9.92×10^6 to 12.03×10^6 copies g^{-1} and did not vary significantly between the farming stages and salinity levels ($p > 0.05$; Fig. 5a). The methanogenic community clearly varied in the pre-farming, farming, and post-farming stages, according to the NMDS and two-way PerMANOVA analyses (Fig. 5b). The major methanogenic genera were *Methanoregula* (~21%), *Methanosaeta* (~16%), *Methanobacterium* (~8%), *Methanospirillum* (~6%), *Methanosarcina* (~6%), *Methanolinea* (~3%), and *Methanococcoides* (~2%), *Methanogenium* (~2%), *Methanosphaera* (~2%), and *Methanocella* (~1%) (Fig. 5c). Other methanogenic genera accounted for less than ~33% of the *mcrA* gene. The relative abundance of *Methanosaeta* was much higher during and after farming than before farming ($p < 0.05$; Fig. 5c).

3.6. Relationships between the methanogenesis, organic substrate, humification indices, and methanogenic community composition

The methanogenesis rates increased with DOC concentrations ($r = 0.77$; $p < 0.001$; $n = 18$), decreased with the C/N ratios ($r = -0.69$; $p < 0.01$; $n = 18$). The *mcrA* gene abundance were not correlated with the methanogenesis rates ($p > 0.05$; $n = 18$). Changes in the humification indices were significantly associated with the $f_{acetoclastic}$ ($p < 0.001$; Figs. 6a to 6d).

The structural equation model suggested that aquaculture farming practices were related to the changes in the methanogenic community composition, while the latter were significantly linked to changes in the methanogenesis pathways (Fig. 7). Aquaculture farming practices also contributed to the changes in the methanogenesis rates (Fig. 7). Salinity was not related to the changes in the methanogenic community composition, whereas negatively related to changes in methanogenesis rates (Fig. 7).

4. Discussion

We analyzed the microbial production of methane and the underlying mechanisms in the sediments of a freshwater and an oligohaline pond before, during, and after shrimp farming. We focused on the effect of farming practices on methanogenesis and the respective contribution

Table 3
Humification indices derived from Fourier-transform infrared spectroscopy (FTIR; means ± standard deviation, n = 3 biological replicates) across three aquaculture farming stages of the freshwater and oligohaline shrimp ponds in the Min River Estuary, southeast China.

FTIR peaks used for humification index*	Ponds	Stages			Factor	Two-way ANOVA		
		Pre-farming	Farming	Post-farming		Stage	Pond	Interaction
1630/1000	Freshwater	0.11 ± 0.01A	0.04 ± 0.01B	0.07 ± 0.01B	***F***	**19.658**	0.044	0.436
	Oligohaline	0.11 ± 0.03A	0.05 ± 0.02B	0.06 ± 0.02B	***P***	**<0.001**	>0.05	>0.05
1740/1000	Freshwater	0.04 ± 0.01A	0.01 ± 0.00B	0.02 ± 0.01B	***F***	**15.755**	0.226	0.204
	Oligohaline	0.05 ± 0.02A	0.01 ± 0.01B	0.02 ± 0.01B	***P***	**<0.001**	>0.05	>0.05
2850/1000	Freshwater	0.10 ± 0.03A	0.02 ± 0.02B	0.04 ± 0.00B	***F***	**13.407**	0.005	0.652
	Oligohaline	0.08 ± 0.03A	0.03 ± 0.02B	0.05 ± 0.02B	***P***	**<0.001**	>0.05	>0.05
2920/1000	Freshwater	0.13 ± 0.03A	0.02 ± 0.02B	0.06 ± 0.00B	***F***	**15.439**	0.107	0.356
	Oligohaline	0.12 ± 0.04A	0.04 ± 0.03B	0.06 ± 0.04B	***P***	**<0.001**	>0.05	>0.05

* FTIR peaks used to generate the humification indices: wavenumbers of lignin or aromatics (1630 cm^{-1}), aromatic esters (1740 cm^{-1}), and aliphatics (2920 cm^{-1} and 2850 cm^{-1}) with respect to polysaccharides (1000 cm^{-1}). References for the wavenumbers are Artz et al. (2008) and Parikh et al. (2014).
Different uppercase letters indicate significant differences across all three farming stages.
Bold letters denote significant differences at $p < 0.05$.

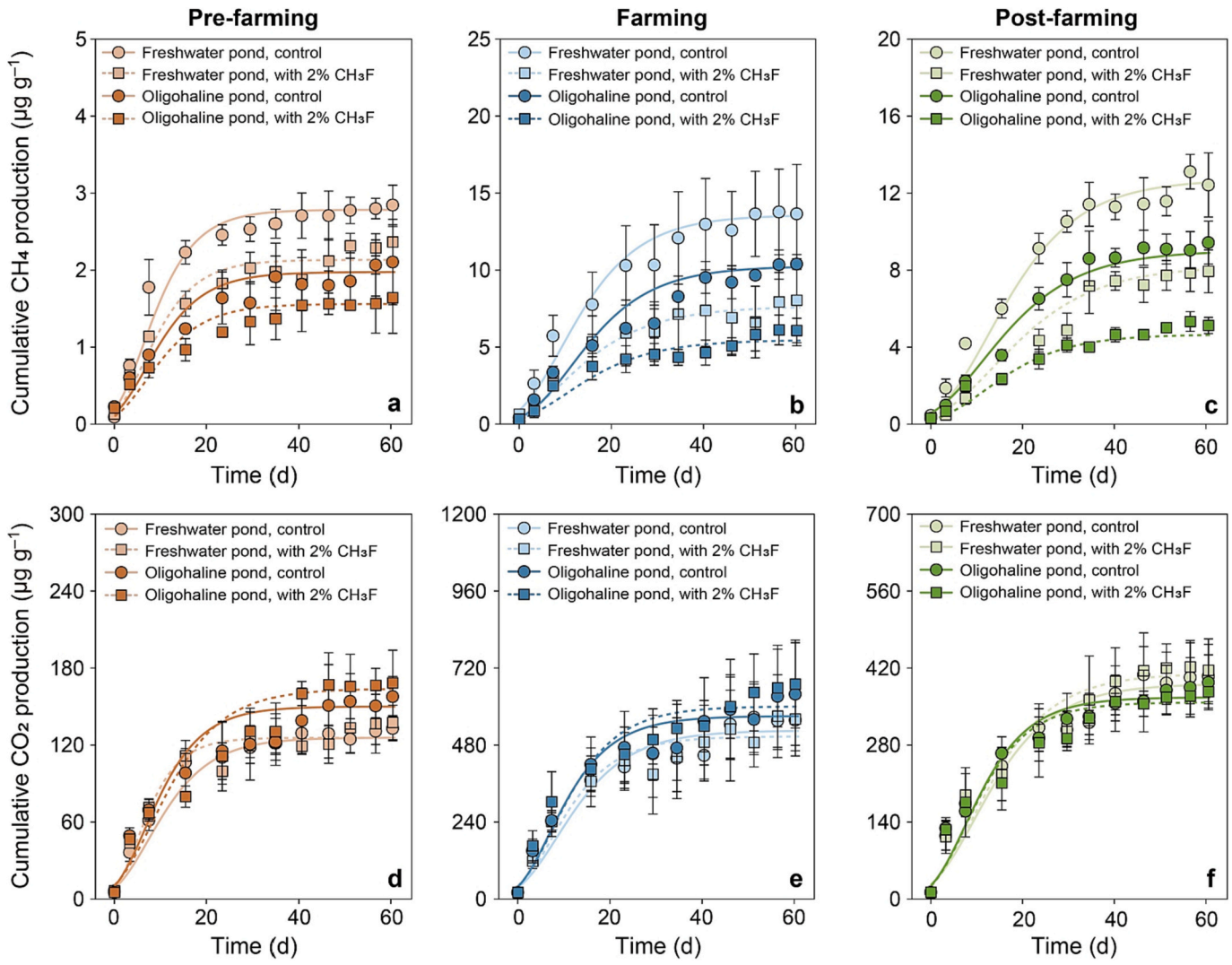

Fig. 2. Cumulative CH_4 and CO_2 production during incubation across three aquaculture farming stages in the sediments of a freshwater and an oligohaline shrimp pond. All data are mean ± standard deviation ($n = 3$ biological replicates). The lines represent the modified Gompertz model curves.

of acetoclastic and hydrogenotrophic methanogenesis.

4.1. *Effect of sediment organic substrate on methanogenesis*

Shrimp aquaculture induced a sharp stimulation in the methanogenesis rates in the sediments at both the farming and post-farming stages compared to the pre-farming stage (Fig. 3a, supporting Hypothesis I). This finding is consistent with previous studies reporting that CH_4 emission fluxes raised during farming in aquaculture ponds (Ma et al., 2018; Song and Liu, 2015; Yang et al., 2018). The raised methanogenesis rates may be due to changes in the quantity and quality of the organic substrate.

The hypothesis that methanogenesis rates is affected by organic substrate quantity, is validated by our results showing that the DOC concentrations increased by an average of 82% during and after farming (Table 2), and were correlated with methanogenesis rates ($r = 0.77$, $p < 0.001$). The high aquafeed loads are typically hydrolyzed to DOC, which is a suitable substrate for methanogens (Olsen et al., 2014; Suhr et al., 2015). Moreover, the production of shrimp excreta is also likely to enrich the DOC in low molecular weight, easily assimilable organic compounds (Queiroz et al., 2019; Wang et al., 2021). Previous research reported similar correlations of methanogenesis rates and DOC concentrations in pristine ponds and paddies (Bertora et al., 2018; Holgerson, 2015).

The effect of the quality of the organic substrate on methanogenesis rates was demonstrated by a high C/N ratio before farming (10.6–11.3), which decreased during and after farming (8.9–9.6), suggesting an input of easily assimilable protein-like nutrients (Panigrahi et al., 2018). A C/N ratio higher than 10.0 is typical of recalcitrant compounds that are not available for benthic microbial metabolism (Baldi et al., 2010; Wei et al., 2022). Decreasing C/N ratios raise the N availability for methanogens and thus accelerate methanogenesis rates (Hou et al., 2022; Kim et al., 2015). Overall, aquaculture farming enhanced methanogenesis rates at the farming and post-farming stages relative to the pre-farming stages by changing the quantity and quality of the organic substrates for the methanogens.

4.2. *Contribution of acetoclastic and hydrogenotrophic methanogenesis*

Acetoclastic and hydrogenotrophic methanogenesis coexisted in the sediments before, during, and after shrimp farming, with a predominance of the hydrogenotrophic pathway by 51%–78% (Figs. 3d to 3f). The rates of the acetoclastic pathway increased by approximately 5.3 times in the sediments at both the farming and post-farming stages compared to the pre-farming stage (Fig. 3e, supporting Hypothesis I). Besides, the contribution of the acetoclastic pathway increased from

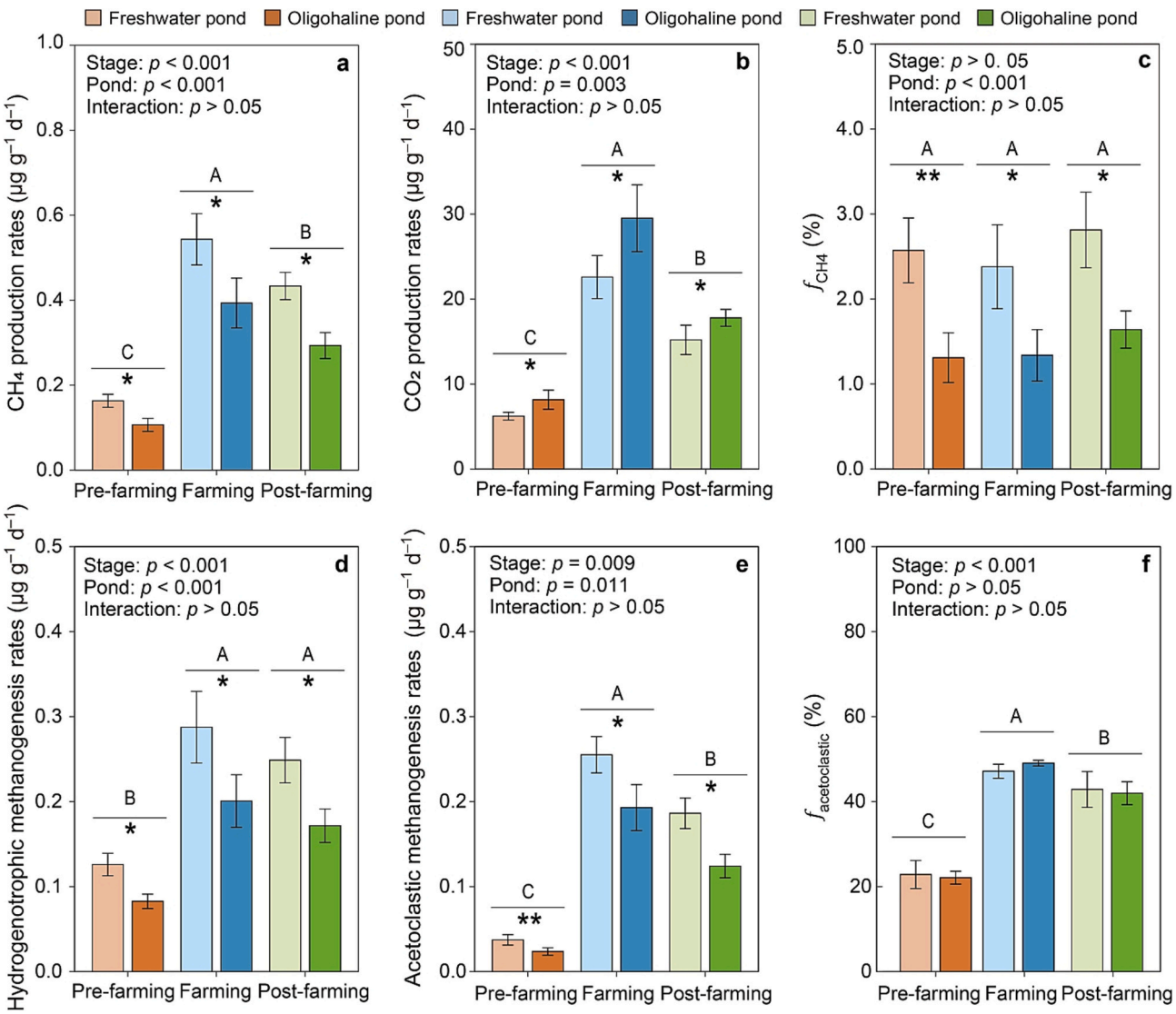

Fig. 3. CH_4 and CO_2 production rates (a and b), f_{CH4} (c), hydrogenotrophic and acetoclastic methanogenesis rates (d and e), and $f_{acetoclastic}$ (f) across three aquaculture farming stages in the sediments of a freshwater and an oligohaline shrimp pond. All data are the mean ± standard deviation (n = 3 biological replicates). Different uppercase letters indicate significant differences across the three aquaculture farming stages. Asterisks denote significant differences between the ponds within one stage (*$p < 0.05$; **$p < 0.01$; ***$p < 0.001$). f_{CH4}: the contribution of CH_4 production rates to the sum production rates of CH_4 plus CO_2. $f_{acetoclastic}$: the contribution of acetoclastic methanogenesis to the CH_4 production rates.

approximately 22% before farming to approximately 45% during and after farming (Fig. 3f). Therefore, aquaculture farming practices favor acetoclastic rather than hydrogenotrophic methanogenesis. The rise of acetoclastic methanogenesis was supported by a decrease in the isotopic fractionation α_c from before farming (1.070–1.074) to during and after farming (1.055–1.062) (Fig. 4c). These values and their corresponding pathways agreed with previous literature (Holmes et al., 2014; Hornibrook et al., 2000). We also observed substantial changes in the composition of the methanogenic community during and after farming (Fig. 5b). In particular, the relative abundance of the acetoclastic methanogen, *Methanosaeta* increased from approximately 9% before farming to approximately 21% during and after farming, confirming the rise of acetoclastic methanogenesis (Fig. 5c).

The shift in the contributions of the different methanogenesis pathways are presumably due to changes in the chemical composition of sediment organic substrate. This is supported by the high association between methanogenesis pathways and the humification indices derived from FTIR (Figs. 6a to 6d). Before farming, the sediments contain relatively stable and recalcitrant organic matter (such as lignin, aromatics, and aliphatics), which cause high humification indices (Table 3). The presence of lignin, aromatics, and aliphatics in sediments agrees with the historical conversion of these vegetated tidal wetlands to ponds as these wetlands are typically dominated by sedge species (Mitsch and Gosselink, 2015). When buried, the plant debris is partially decomposed, leaving lignin, aliphatics, and other complex compounds (Berberich et al., 2020; Gleixner, 2013; Lichtfouse, 1999; Martínez-García et al., 2018). These recalcitrant compounds can partly be oxidized to produce H_2 (Conrad et al., 2010a; Keller et al., 2004), thus favoring hydrogenotrophic methanogenesis.

During and after farming, the amounts of aquafeed were added into the ponds. Indeed, 30% of aquafeed is not captured by shrimps, and settles in the sediment (Soto, 2021). The aquafeed was mainly composed of peanut and bean dregs, which are rich in polysaccharides (Dawood et al., 2018). Consequently, the humification indices decreased during and after farming due to the high relative abundance of polysaccharides (Table 3). Rawoof et al. (2020) stated that polysaccharide hydrolysis produces glucose, fructose, and xylose, which are further biodegraded into acetate, thus stimulating acetoclastic methanogens. The stimulation

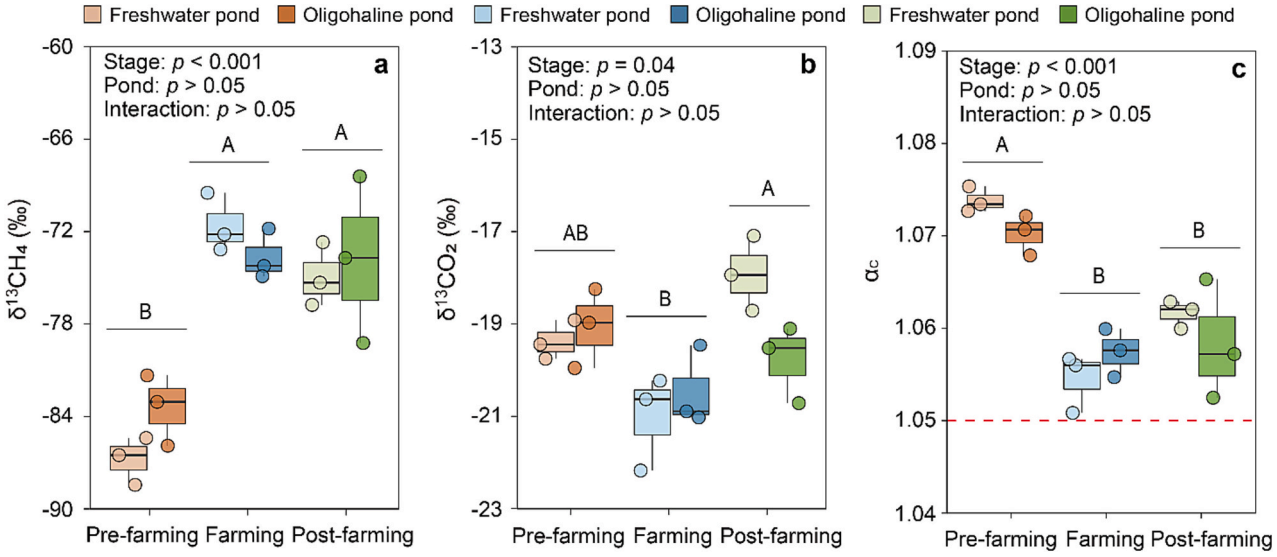

Fig. 4. $\delta^{13}CH_4$ and $\delta^{13}CO_2$ values (mean ± standard deviation; n = 3 biological replicates) of the sediment at the completion of a 60 d-incubation across three aquaculture farming stages of a freshwater and an oligohaline shrimp pond. Different uppercase letters indicate significant differences across the three aquaculture farming stages. Asterisks denote significant difference between ponds within a single stage (*$p < 0.05$; **$p < 0.01$; ***$p < 0.001$). The red line in panel c provides the separation between the relative importance of hydrogenotrophic (above) and acetoclastic (below) methanogenesis (Whiticar, 1999). (For interpretation of the references to colour in this figure legend, the reader is referred to the web version of this article.)

of acetoclastic methanogenesis by labile C has also been suggested in peat (Keller and Bridgham, 2007). Our previous study also showed acetoclastic methanogenesis was feasible when there were high concentrations of polysaccharides in anaerobic soils (Xiao et al., 2019). Overall, aquaculture farming favored acetoclastic over hydrogenotrophic methanogenesis, because of the input of polysaccharide-rich aquafeeds.

4.3. Effect of salinity on methanogenesis

The methanogenesis rates were lower in the oligohaline pond than the freshwater pond (Fig. 3a). Salinity is known to control the methanogenic community by increasing ionic toxicity and altering the osmotic potential (Luo et al., 2019; Tully et al., 2019). Nonetheless, the abundance of the *mcrA* gene was not significantly different between the oligohaline and freshwater ponds (Fig. 5a). The results are probably due to the major methanogenic genera, e.g., *Methanoregula*, *Methanosaeta*, *Methanobacterium*, *Methanospirillum,* and *Methanosarcina* are all frequently encountered methanogenic taxa in estuaries where salinity is high (ranging from 5‰ to 20‰) (Chen et al., 2019; Liu et al., 2016; Tong et al., 2017). Therefore, salt stress is probably not the cause of the lower methanogenesis rates in the oligohaline pond relative to the freshwater pond (against Hypothesis II).

A more probable explanation is the sulfate reduction in the oligohaline pond yields a stronger Gibbs free energy compared to methanogenesis, and therefore inhibits methanogen activities (Herbert et al., 2015). This assumption is supported by the sulfate concentrations, these are approximately 10-times higher in the oligohaline pond compared to the freshwater pond (Table 2). Moreover, sulfate-reducing bacteria can oxidize CH_4 to CO_2 under anaerobic conditions (Rotaru and Thamdrup, 2016; Wilms et al., 2007), which could also explain the lower methanogenesis rates in the oligohaline pond.

While both hydrogenotrophic and acetoclastic pathways displayed lower methanogenesis rates in the oligohaline when compared to the freshwater pond (Fig. 3d), their respective contributions were similar (Fig. 3f). Similarly, the isotopic fractionation factor α_c and the methanogenic community composition did not differ between the two ponds (Figs. 4c and 5b). These findings suggest salinity did not alter the partitioning of the methanogenesis pathways. A previous study suggested that salinity may change methanogenesis pathways due to the different relative salt-tolerances of the hydrogenotrophic and acetoclastic methanogens (Liu et al., 2016). However, the dominated hydrogenotrophic and acetoclastic methanogens were both tolerant to low-salinity as discussed before. Therefore, salinity differences between the ponds did not lead to different partitioning of methanogenesis pathways in the current study.

4.4. Implication for how aquaculture management can reduce methane emission in the future

First, we revealed the rise of acetoclastic versus hydrogenotrophic methanogenesis in shrimp farming. This rise is explained by the input of aquafeeds increasing the proportions of labile, microbially assimilable organic compounds, such as polysaccharides. Using this knowledge, we suggest changing shrimp diets, similarly to cow farming to better control and possibly reduce methane emissions (Hassanat et al., 2013; Marette and Millet, 2014). For instance, the addition of oilseeds (camelina and safflower) may not influence the growth of aquaculture products; however, these lipid-rich feeds have a toxic effect on the activities of archaea, which would further reduce methanogen abundance (Wang et al., 2017).

Second, our results reported that the lower rates of methanogenesis in the oligohaline pond are because of the inhibition of sulfate reduction and oxidation of CH_4 to CO_2 by sulfate in anaerobic conditions. Based on this conclusion, we suggested that freshwater shrimp aquaculture ponds would benefit from moderate salt levels. The addition of moderate salt (salinity = 2.5‰) into ponds had been applied in carp freshwater aquaculture systems in India, which was found to stimulate the growth of the fish and greatly suppress CH_4 emissions (Naskar et al., 2020). *L. vannamei* is a euryhaline shrimp species, which could grow well in ponds with salinity of 0‰ to 30‰ (Jannathulla et al., 2017). Therefore, the addition of salt in the freshwater ponds would not influence the growth of the shrimps; however, it would greatly decrease the CH_4 emissions.

Third, we have found that methanogenesis maintained high-levels even after farming. This was because the amounts of aquafeed residues deposited on the pond sediments. Therefore, an effective way to reduce methanogenesis in aquaculture ponds was to clean aquafeed

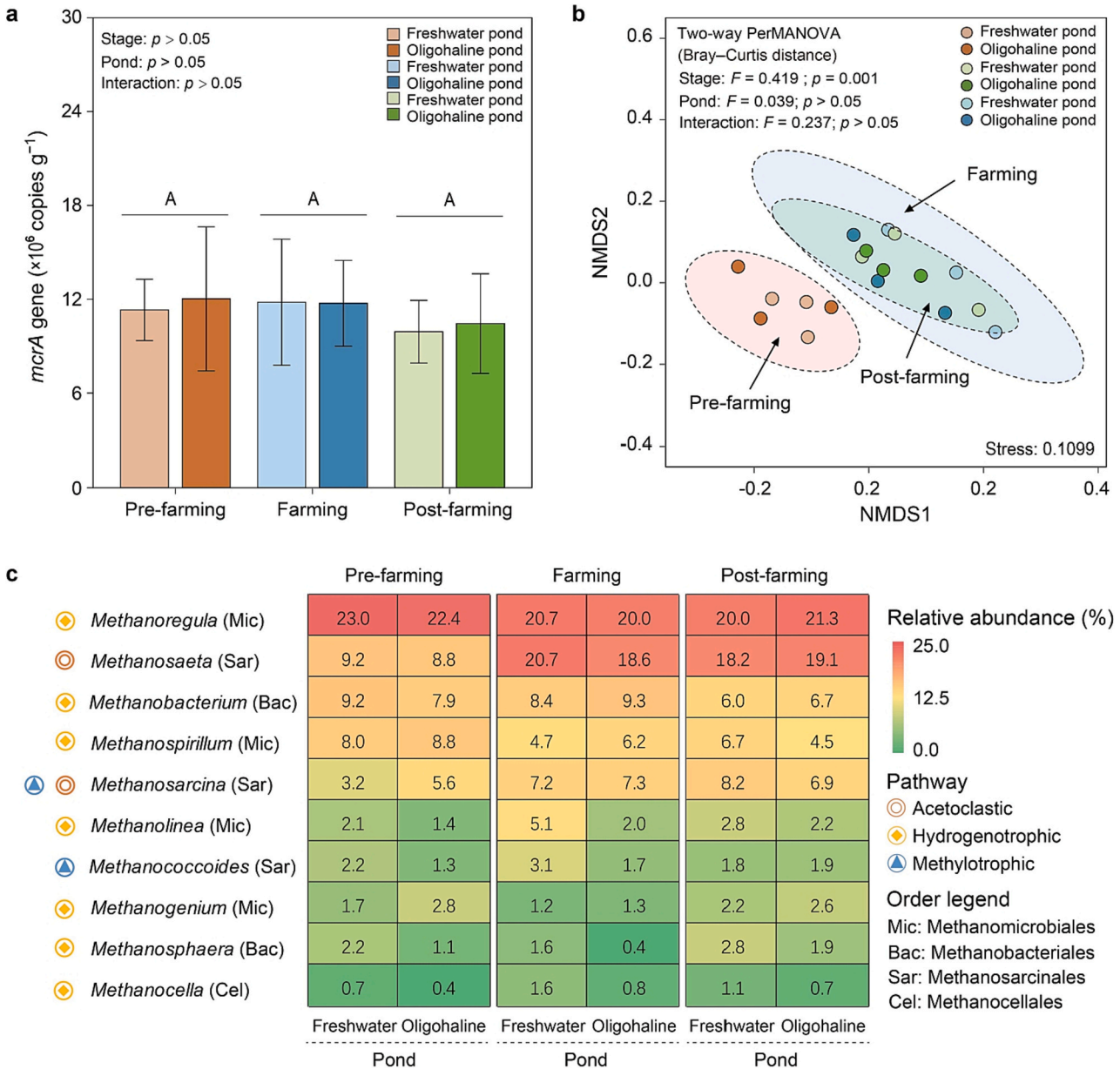

Fig. 5. Graphical representations of the methanogenic community structure variations in three aquaculture farming stages of a freshwater and an oligohaline shrimp pond. (a) The abundance of *mcrA* gene (mean ± standard deviation, n = 3 biological replicates). (b) The nonmetric multidimensional scaling (NMDS) plot of the methanogenic community composition (n = 3 biological replicates). and (c) A heatmap demonstrating the relative abundance of methanogen genera. Different uppercase letters in panel a indicate significant differences across the three aquaculture farming stages.

residues (Chik et al., 2017). Once the farming activities are completed, the pond water should be drained and the aquafeed residues should be removed immediately to reduce the potential of methanogenesis.

5. Conclusions

This study reveals shrimp farming increases the acetoclastic methanogenesis when compared to hydrogenotrophic methanogenesis in a pond. This is due to the input of polysaccharide-rich aquafeed and shrimp excreta increasing the levels of fresh organic matter in the pond sediments. The methanogenesis rate is lower in the oligohaline pond than freshwater pond. Salinity did not change the relative composition of the methanogenic community or modify the respective contribution of the acetoclastic and hydrogenotrophic methanogenesis. In the future, methanogenesis in shrimp ponds could be reduced by changing shrimp diets, increasing salinity, and removing residual aquafeeds.

Author contributions

Luo and Xiao designed the experiment. Luo and Tan co-wrote the manuscript with substantial contributions from Lichtfouse. Tan, Zhang, Chen, Liu and Huang did the scientific analysis. All authors conducted the research and analyzed data. All authors edited the manuscript.

Data availability statement

Data deposited in the figshare, https://figshare.com/s/a081915a95654a76efd0. Raw *mcrA* gene sequence reads for each sample are also available on NCBI Short Read Archive (SRA) under the BioProject number PRJNA532292.

CRediT authorship contribution statement

Ji Tan: Investigation, Writing – original draft. **Eric Lichtfouse:**

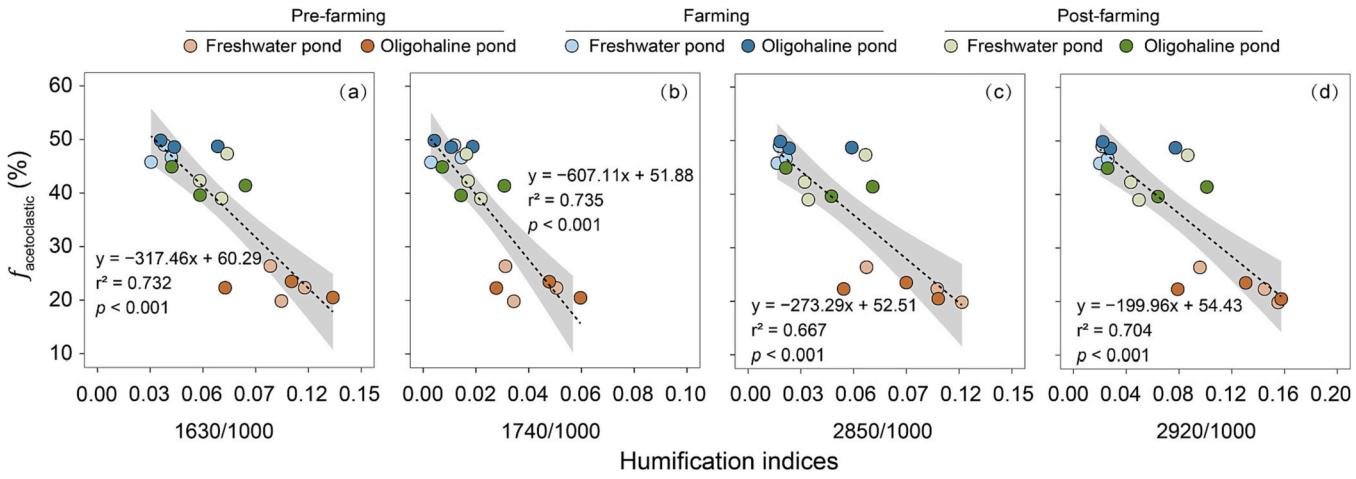

Fig. 6. Relationships between humification indices and the $f_{acetoclastic}$. Humification indices are derived from Fourier-transform infrared spectroscopy. $f_{acetoclastic}$: the contribution of acetoclastic methanogenesis to the CH_4 production rates.

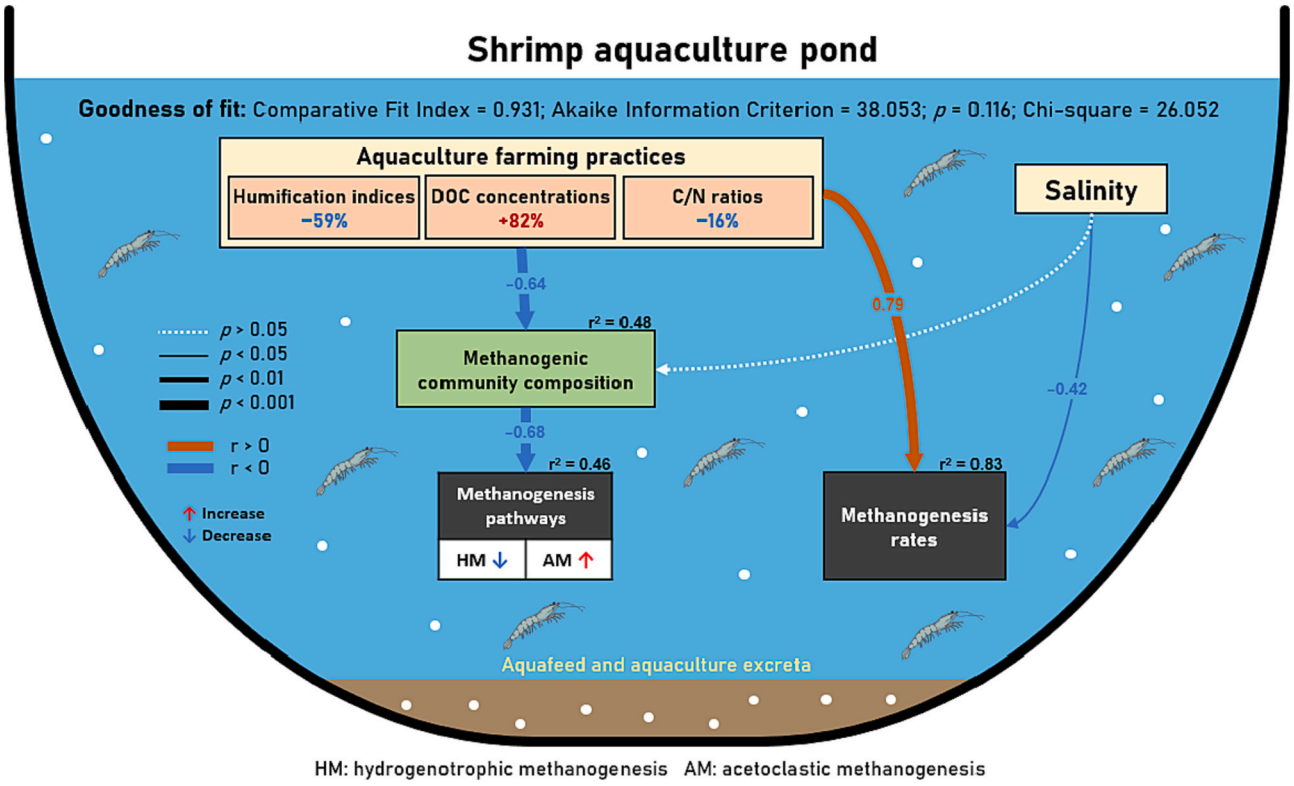

Fig. 7. A structural equation modelling accessing the impact of aquaculture farming practices and salinity on rates and pathways of methanogenesis. Numbers on the arrows indicate the coefficients and the arrow width indicates their significance. Figures next to the variables indicate their explained variance (r^2). DOC: dissolved organic carbon; HM: hydrogenotrophic methanogenesis; AM: acetoclastic methanogenesis.

Writing – review & editing. **Min Luo:** Conceptualization, Methodology, Writing – review & editing, Supervision, Project administration. **Fengfeng Tan:** Investigation, Formal analysis. **Changwei Zhang:** Investigation, Formal analysis. **Jiafang Huang:** Investigation, Formal analysis. **Leilei Xiao:** Conceptualization, Methodology.

Declaration of Competing Interest

The authors declare that they have no known competing financial interests or personal relationships that could have appeared to influence the work reported in this paper.

Data availability

Data deposited in the figshare, https://figshare.com/s/a081915a95654a76efd0. Raw mcrA gene sequence reads are also available on NCBI Short Read Archive (SRA) under the BioProject number PRJNA532292.

Acknowledgments

This work was financially supported by grants from the National Science Foundation of China (No. 32071598; 42077025; 41671088), the Natural Science Foundation of Fujian Province (No. 2020J01503), the

Science and Technology Projects of the Forest Bureau of Fujian Province (No. 2021FKJ30), and Youth Innovation Promotion Association, CAS (2021213).

Appendix A. Supplementary data

Supplementary data to this article can be found below and online at https://doi. org/10.1016/j.aquaculture.2022.738999.

References

Ali, G., Ling, Z., Saif, I., Usman, M., Jalalah, M., Harraz, F.A., Al-Assiri, M.S., Salama, El-S, Li, X., 2021. Biomethanation and microbial community response during agricultural biomass and shrimp chaff digestion. Environ. Pollut. 278, 116801 https://doi.org/10.1016/j.envpol.2021.116801.

Artz, R.R., Chapman, S.J., Robertson, A.J., Potts, J.M., Laggoun-Défarge, F., Gogo, S., Comont, L., Disnar, J.R., Francez, A.J., 2008. FTIR spectroscopy can be used as a screening tool for organic matter quality in regenerating cutover peatlands. Soil Biol. Biochem. 40 (2), 515–527. https://doi.org/10.1016/j.soilbio.2007.09.019.

Baldi, F., Marchetto, D., Pini, F., Fani, R., Giani, M., 2010. Biochemical and microbial features of shallow marine sediments along the Terra Nova Bay (Ross Sea, Antarctica). Cont. Shelf Res. 30 (15), 1614–1625. https://doi.org/10.1016/j.csr.2010.06.009.

Beer, J., Lee, K., Whiticar, M., Blodau, C., 2008. Geochemical controls on anaerobic organic matter decomposition in a northern peatland. Limnol. Oceanogr. 53 (4), 1393–1407. https://doi.org/10.2307/40058261.

Berberich, M.E., Beaulieu, J.J., Hamilton, T.L., Wald Limn, O., S., Buffam, I., 2020. Spatial variability of sediment methane production and methanogen communities within a eutrophic reservoir: importance of organic matter source and quantity. Limnol. Oceanogr. 65 (6), 1–23. https://doi.org/10.1002/lno.11392.

Bertora, C., Cucu, M.A., Lerda, C., Peyron, M., Bardi, L., Gorra, R., Sacco, D., Celi, L., Said-Pullicino, D., 2018. Dissolved organic carbon cycling, methane emissions and related microbial populations in temperate rice paddies with contrasting straw and water management. Agric. Ecosyst. Environ. 265, 292–306. https://doi.org/10.1016/j.agee.2018.06.004.

Bräuer, S.L., Cadillo-Quiroz, H., Ward, R.J., Yavitt, J.B., Zinder, S.H., 2011. *Methanoregula boonei* gen. nov., sp. nov., an acidiphilic methanogen isolated from an acidic peat bog. Int J Syst Evol Microbiol 61, 45–52. https://doi.org/10.1099/ijs.0.021782-0.

Caporaso, J.G., Lauber, C.L., Walters, W.A., Berg-Lyons, D., Huntley, J., Fierer, N., Owens, S.M., Betley, J., Fraser, L., Bauer, M., Gormley, N., Gilbert, J.A., Smith, G., Knight, R., 2012. Ultra-high-throughput microbial community analysis on the Illumina HiSeq and MiSeq platforms. ISME J 6, 1621–1624. https://doi.org/10.1038/ismej.2012.8.

Chambers, L.G., Osborne, T.Z., Reddy, K.R., 2013. Effect of salinity-altering pulsing events on soil organic carbon loss along an intertidal wetland gradient: a laboratory experiment. Biogeochemistry 115 (1), 363–383. https://doi.org/10.1007/s10533-013-9841-5.

Chen, H., Chang, S., 2020. Dissecting methanogenesis for temperature-phased anaerobic digestion: impact of temperature on community structure, correlation, and fate of methanogens. Bioresour. Technol. 306, 123104 https://doi.org/10.1016/j.biortech.2020.123104.

Chen, Y., Dong, S., Wang, Z., Wang, F., Cao, Q.F., Tian, X.L., Xiong, Y.H., 2015. Variations in CO_2 fluxes from grass carp *Ctenopharyngodon idella* aquaculture polyculture ponds. Aquacult. Env. Interac. 8, 31–40. https://doi.org/10.3354/aei00149.

Chen, S., Wang, P., Liu, H., Xie, W., Sean Wan, X., Kao, S., Phelps, T.J., Zhang, C., 2020. Population dynamics of methanogens and methanotrophs along the salinity gradient in Pearl River Estuary: implications for methane metabolism. Appl. Microbiol. Biotechnol. 104 (3), 1331–1346. https://doi.org/10.1007/s00253-019-10221-6.

Chen, S., Wang, P., Liu, H., Xie, W., Wan, X.S., Kao, S.J., Phelps, T.J., Zhang, C., 2019. Population dynamics of methanogens and methanotrophs along the salinity gradient in Pearl River estuary: implications for methane metabolism. Appl. Microbiol. Biotechnol. 104, 1331–1346. https://doi.org/10.1007/s00253-019-10221-6.

Chik, M.N., Yahya, L., Zainal, A., Boosroh, M.H., 2017. Microalgae and its premises towards sustainable energy development. IOP Conf. Ser.: Mater. Sci. Eng. 206, 012022 https://doi.org/10.1088/1757-899X/206/1/012022.

Conrad, R., 1999. Contribution of hydrogen to methane production and control of hydrogen concentrations in methanogenic soils and sediments. FEMS Microbiol. Ecol. 28, 193–202. https://doi.org/10.1016/S0168-6496(98)00086-5.

Conrad, R., 2005. Quantification of methanogenic pathways using stable carbon isotopic signatures: a review and a proposal. Org. Geochem. 36, 739–752. https://doi.org/10.1016/j.orggeochem.2004.09.006.

Conrad, R., Chan, O.C., Claus, P., Casper, P., 2007. Characterization of methanogenic archaea and stable isotope fractionation during methane production in the profundal sediment of an oligotrophic Lake (lake Stechlin, Germany). Limnol. Oceanogr. 52 (4), 1393–1406. https://doi.org/10.4319/lo.2007.52.4.1393.

Conrad, R., Claus, P., Casper, P., 2010a. Stable isotope fractionation during the methanogenic degradation of organic matter in the sediment of an acidic bog lake Lake Grosse Fuchskuhle. Limnol. Oceanogr. 55 (5), 1932–1942. https://doi.org/10.4319/lo.2010.55.5.1932.

Conrad, R., Klose, M., Claus, P., Enrich-Prastb, A., 2010b. Methanogenic pathway, ^{13}C isotope fractionation, and archaeal community composition in the sediment of two clear-water lakes of Amazonia. Limnology Limnol. Oceanogr. 55 (2), 689–702. https://doi.org/10.1002/jgrg.20055.

Conrad, R., Klose, M., Enrich-Prast, A., 2020. Acetate turnover and methanogenic pathways in Amazonian lake sediments. Biogeosciences 17 (4), 1063–1069. https://doi.org/10.5194/bg-17-1063-2020.

Corbett, J.E., Tfaily, M.M., Burdige, D.J., Glaser, P.H., Chanton, J.P., 2015. The relative importance of methanogenesis in the decomposition of organic matter in northern peatlands. J. Geophys. Res. Biogeosci. 120 (2), 280–293. https://doi.org/10.1002/2014JG002797.

Cui, B., He, Q., Gu, B., Bai, J., Liu, X., 2016. China's coastal wetlands: understanding environmental changes and human impacts for management and conservation. Wetlands 36 (1), 1–9. https://doi.org/10.1007/s13157-016-0737-8.

Dawood, M.A.O., Koshio, S., Esteban, M.Á., 2018. Beneficial roles of feed additives as immunostimulants in aquaculture: a review. Rev. Aquac. 10 (4), 950–974. https://doi.org/10.1111/raq.12209.

Dridi, B., Fardeau, M.L., Ollivier, B., Raoult, D., Drancourt, M., 2012. *Methanomassiliicoccus luminyensis* gen. Nov., sp. nov., a methanogenic archaeon isolated from human faeces. Int. J. Syst. Evol. Microbiol. 62 (8), 1902–1907. https://doi.org/10.1099/ijs.0.033712-0.

Etminan, M., Myhre, G., Highwood, E.J., Shine, K.P., 2016. Radiative forcing of carbon dioxide, methane, and nitrous oxide: a significant revision of the methane radiative forcing. Geophys. Res. Lett. 43 (24) https://doi.org/10.1002/2016GL071930.

European Union Commission, 2021. Launch by US, EU and Partners of the Global Methane Pledge. Available online. https://ec.europa.eu/commission/presscorner/detail/en/statement_21_5766.

FAO, 2018. The State of World Fisheries and Aquaculture 2018-Meeting the Sustainable Development Goals. Food and Agricultural Organization, pp. 1–210.

Gleixner, G., 2013. Soil organic matter dynamics: a biological perspective derived from the use of compound-specific isotopes studies. Ecol. Res. 28 (5), 683–695. https://doi.org/10.1007/s11284-012-1022-9.

Gotelli, N.J., Colwell, R.K., 2001. Quantifying biodiversity: procedures and pitfalls in the measurement and comparison of species richness. Ecol. Lett. 4 (4), 379. https://doi.org/10.1046/j.1461-0248.2001.00230.x.

Hassanat, F., Gervais, R., Julien, C., Massé, D.I., Lettat, A., Chouinard, P.Y., Petit, H.V., Benchaar, C., 2013. Replacing alfalfa silage with corn silage in dairy cow diets: effects on enteric methane production, ruminal fermentation, digestion, N balance, and milk production. J. Dairy Sci. 96 (7), 4553–4567.

Herbert, E.R., Boon, P., Burgin, A.J., Neubauer, S.C., Franklin, R.B., Ardón, M., Hopfensperger, K.N., Lamers, L.P.M., Gell, P., 2015. A global perspective on wetland salinization: ecological consequences of a growing threat to freshwater wetlands. Ecosphere 6 (10), 1–43. https://doi.org/10.1890/ES14-00534.1.

Hines, M.E., Duddleston, K.N., Rooney-Varga, J.N., Fields, D., Chanton, J.P., 2008. Uncoupling of acetate degradation from methane formation in Alaskan wetlands: connections to vegetation distribution. Glob. Biogeochem. Cycles 22 (2), GB2017. https://doi.org/10.1029/2006GB002903.

Hodgkins, S.B., Tfaily, M.M., McCalley, C.K., Logan, T.A., Crill, P.M., Saleska, S.R., Rich, V.I., Chanton, J.P., 2014. Changes in peat chemistry associated with permafrost thaw increase greenhouse gas production. PNAS 111 (16), 5819–5824. https://doi.org/10.1073/pnas.1314641111.

Hofmann, K., Praeg, N., Mutschlechner, M., Wagner, A.O., Illmer, P., 2016. Abundance and potential metabolic activity of methanogens in well-aerated forest and grassland soils of an alpine region. FEMS Microbiol. Ecol. 92 (2) https://doi.org/10.1093/femsec/fiv171.

Holgerson, M.A., 2015. Drivers of carbon dioxide and methane supersaturation in small, temporary ponds. Biogeochemistry 124 (1), 305–318. https://doi.org/10.1007/s10533-015-0099-y.

Holmes, M.E., Chanton, J.P., Bae, H.-S., Ogram, A., 2014. Effect of nutrient enrichment on $\delta^{13}CH_4$ and the methane production pathway in the Florida Everglades. J. Geophys. Res. Biogeosci. 119 (7), 1267–1280. https://doi.org/10.1002/jgrg.20122.

Holmes, M.E., Chanton, J.P., Tfaily, M.M., Ogram, A., 2015. CO_2 and CH_4 isotope compositions and production pathways in a tropical peatland. Global Biogeochem Cycles 29 (1), 1–18. https://doi.org/10.1002/2014GB004951.

Hornibrook, E.R.C., Longstaffe, F.J., Fyfe, W.S., 2000. Evolution of stable carbon isotope compositions for methane and carbon dioxide in freshwater wetlands and other anaerobic environments. Geochim. Cosmochim. Acta 64 (6), 1013–1027. https://doi.org/10.1016/S0016-7037(99)00321-X.

Hou, L., Zheng, Y., Liu, M., Gong, J., Zhang, X., Yin, G., You, L., 2013. Anaerobic ammonium oxidation (anammox) bacterial diversity, abundance, and activity in marsh sediments of the Yangtze estuary. J. Geophys. Res. Biogeosci. 118 (3), 1237–1246. https://doi.org/10.1002/jgrg.20108.

Hou, P., Xue, L., Wang, J., Petropoulos, E., Deng, X., Qiao, J., Xue, L., Yang, L., 2022. Continuous milk vetch amendment in rice-fallow rotation improves soil fertility and maintains rice yield without increasing CH_4 emissions: evidence from a long-term experiment. Agric. Ecosyst. Environ. 325 https://doi.org/10.1016/j.agee.2021.107774.

IPCC, 2021. Climate Change 2021: The Physical Science Basis. Contribution of Working Group I to the Sixth Assessment Report of the Intergovernmental Panel on Climate Change. Cambridge University Press. In Press. https://www.ipcc.ch/report/sixth-assessment-report-working-group-i/.

Jannathulla, R., Dayal, J.S., Chitra, V., Ambashankar, K., Murlidhar, M., 2017. Growth and carcass mineralisation of Pacific white leg shrimp *Penaeus vannamei* Boone 1931 in response to water salinity. Indian J. Fish. 64 (2), 40–47. https://doi.org/10.21077/ijf.2017.64.2.60341-07.

Ji, Y., Liu, P., Conrad, R., 2018. Change of the pathway of methane production with progressing anoxic incubation of paddy soil. Soil Biol. Biochem. 121, 177–184. https://doi.org/10.1016/j.soilbio.2018.03.014.
Keller, J.K., Bridgham, S.D., 2007. Pathways of anaerobic carbon cycling across an ombrotrophic–minerotrophic peatland gradient. Limnol. Oceanogr. 52, 96–107. https://doi.org/10.4319/lo.2007.52.1.0096.
Keller, J.K., White, J.R., Bridgham, S.D., Pastor, J., 2004. Climate change effects on carbon and nitrogen mineralization in peatlands through changes in soil quality. Glob. Chang. Biol. 10 (7), 1053–1064. https://doi.org/10.1111/j.1529-8817.2003.00785.x.
Kim, S.Y., Veraart, A.J., Meima-Franke, M., Bodelier, P.L.E., 2015. Combined effects of carbon, nitrogen and phosphorus on CH_4 production and denitrification in wetland sediments. Geoderma 259, 354–361. https://doi.org/10.1016/j.geoderma.2015.03.015.
King, G.M., Klug, M.J, Lovely, D.R., 1983. Metabolism of acetate , methanol , and methylated amines in intertidal sediments of Lowes Cove, Maine. Appl. Environ. Microbiol. 45, 1848–1853. https://doi.org/10.1128/aem.45.6.1848-1853.1983.
Kotsyurbenko, O.R., Chin, K.J., Glagolev, M.V., Stubner, S., Simankova, M.V., Nozhevnikova, A.N., Conrad, R., 2004. Acetoclastic and hydrogenotrophic methane production and methanogenic populations in an acidic west-Siberian peat bog. Environ. Microbiol. 6 (11), 1159–1173. https://doi.org/10.1111/j.1462-2920.2004.00634.x.
Krohn, J., Lozanovska, I., Kuzyakov, Y., Parvin, S., Dorodnikov, M., 2017. CH_4 and CO_2 production below two contrasting peatland micro-relief forms: an inhibitor and $\delta^{13}C$ study. Sci. Total Environ. 586, 142–151. https://doi.org/10.1016/j.scitotenv.2017.01.192.
Li, J., Xiao, L., Zheng, S., Zhang, Y., Luo, M., Tong, C., Xu, H., Tan, Y., Liu, J., Wang, O., Liu, F., 2018. A new insight into the strategy for methane production affected by conductive carbon cloth in wetland soil: beneficial to acetoclastic methanogenesis instead of CO_2 reduction. Sci. Total Environ. 643, 1024–1030. https://doi.org/10.1016/j.scitotenv.2018.06.271.
Lichtfouse, E., 1999. A novel model of humin. Analusis 27 (5), 385–386. https://hal.archives-ouvertes.fr/hal-00262443.
Liu, Y., Whitman, W.B., 2008. Metabolic, phylogenetic, and ecological diversity of the methanogenic archaea. Ann. N. Y. Acad. Sci. 1125 (1), 171–189. https://doi.org/10.1196/annals.1419.019.
Liu, D., Ding, W., Jia, Z., Cai, Z., 2012. The impact of dissolved organic carbon on the spatial variability of methanogenic archaea communities in natural wetland ecosystems across China. Appl. Microbiol. Biotechnol. 96, 253–263. https://doi.org/10.1007/s00253-011-3842-x.
Liu, Y., Priscu, J.C., Xiong, J., Conrad, R., Vick-Majors, T., Chu, H., Hou, J., 2016. Salinity drives archaeal distribution patterns in high altitude lake sediments on the Tibetan plateau. FEMS Microbiol. Ecol. 92, 3. https://doi.org/10.1093/femsec/fiw033.
Luo, M., Zhu, W., Huang, J., Liu, Y., Duan, X., Wu, J., Tong, C., 2019. Anaerobic organic carbon mineralization in tidal wetlands along a low-level salinity gradient of a subtropical estuary: rates, pathways, and controls. Geoderma 337, 1245–1257. https://doi.org/10.1016/j.geoderma.2018.07.030.
Ma, Y., Sun, L., Liu, C., Yang, X., Zhou, W., Yang, B., Schwenke, G., Liu, L., 2018. A comparison of methane and nitrous oxide emissions from inland mixed-fish and crab aquaculture ponds. Sci. Total Environ. 637, 517–523. https://doi.org/10.1016/j.scitotenv.2018.05.040.
Mach, V., Blaser, M.B., Claus, P., Chaudhary, P.P., Rulik, M., 2015. Methane production potentials, pathways, and communities of methanogens in vertical sediment profiles of river Sitka. Front. Microbiol. 6, 506. https://doi.org/10.3389/fmicb.2015.00506.
Magondu, E.W., Charo-Karisa, H., Verdegem, M.C.J., 2013. Effect of C/N ratio levels and stocking density of Labeo victorianus on pond environmental quality using maize flour as a carbon source. Aquaculture 410, 157–163. https://doi.org/10.1016/j.aquaculture.2013.06.021.
Mandic-Mulec, I., Gorenc, K., Gams, M., Petrišič, M.G., Faganeli, J., Ogrinc, N., 2012. Methanogenesis pathways in a stratified eutrophic alpine lake (Lake Bled, Slovenia). Limnol. Oceanogr. 57 (3), 868–880. https://doi.org/10.4319/lo.2012.57.3.0868.
Marette, S., Millet, G., 2014. Economic benefits from promoting linseed in the diet of dairy cows for reducing methane emissions and improving milk quality. Food Policy 46, 140–149. https://doi.org/10.1016/j.foodpol.2014.03.010.
Martínez-García, L.B., Korthals, G., Brussaard, L., Jørgensen, H.B., De Deyn, G.B., 2018. Organic management and cover crop species steer soil microbial community structure and functionality along with soil organic matter properties. Agric. Ecosyst. Environ. 263, 7–17. https://doi.org/10.1016/j.agee.2018.04.018.
Mitsch, W.J., Gosselink, J.G., 2015. Wetlands, 5th ed. John Wiley & Sons, Inc, pp. 259–310.
Mulat, D.G., Jacobi, H.F., Feilberg, A., Adamsen, A.P.S., Richnow, H.H., Nikolausz, M., 2016. Changing feeding regimes to demonstrate flexible biogas production: effects on process performance, microbial community structure, and methanogenesis pathways. Appl. Environ. Microbiol. 82 (2), 438–449. https://doi.org/10.1128/AEM.02320-15.
Naskar, S., Pailan, G.H., Datta, S., Sawant, P.B., Bharti, V.S., 2020. Effect of different organic manures and salinity levels on greenhouse gas emission and growth of common carp in aquaculture systems. Aquac. Res. 00, 1–10. https://doi.org/10.1111/are.15041.
Naylor, R.L., Hardy, R.W., Buschmann, A.H., Bush, S.R., Cao, L., Klinger, D.H., Little, D. C., Lubchenco, J., Shumway, S.E., Troell, M., 2021. A 20-year retrospective review of global aquaculture. Nature 591 (7851), 551–563. https://doi.org/10.1038/s41586-021-03308-6.
Neubauer, S.C., Franklin, R.B., Berrier, D.J., 2013. Saltwater intrusion into tidal freshwater marshes alters the biogeochemical processing of organic carbon. Biogeosciences 10 (12), 8171–8183. https://doi.org/10.5194/bg-10-8171-2013.
Neubauer, S.C., Megonigal, J.P., 2015. Moving beyond global warming potentials to quantify the climatic role of ecosystems. Ecosystems 18 (6), 1000–1013. https://doi.org/10.1007/s10021-015-9879-4.
Olsen, L.M., Holmer, M., Olsen, Y., 2014. Perspectives of nutrient emission from fish aquaculture in coastal waters: literature review with evaluated state of knowledge. FHF Project 542014, 87. https://doi.org/10.13140/RG.2.1.1273.8006.
Panigrahi, A., Saranya, C., Sundaram, M., Vinoth Kannan, S.R., Das Rasmi, R., Satish Kumar, R., Rajesh, P., Otta, S.K., 2018. Carbon:Nitrogen (C:N) ratio level variation influences microbial community of the system and growth as well as immunity of shrimp (*Litopenaeus vannamei*) in biofloc based culture system. Fish Shellfish Immunol. 81, 329–337. https://doi.org/10.1016/j.fsi.2018.07.035.
Parikh, S.J., Mukome, F., Zhang, X., 2014. Atr-ftir spectroscopic evidence for biomolecular phosphorus and carboxyl groups facilitating bacterial adhesion to iron oxides. Colloids Surf B 119, 38–46. https://doi.org/10.1016/j.colsurfb.2014.04.022.
Penger, J., Conrad, R., Blaser, M., 2012. Stable carbon isotope fractionation by methylotrophic methanogenic archaea. AEM 78 (21), 7596–7602. https://doi.org/10.1128/AEM.01773-12.
Pusceddu, A., Della Patrona, L., Beliaeff, B., 2011. Trophic status of earthen ponds used for semi-intensive shrimp (*Litopenaeus stylirostris*, Stimpson, 1874) farming in New Caledonia (Pacific Ocean). Mar. Environ. Res. 72 (4), 160–171. https://doi.org/10.1016/j.marenvres.2011.07.005.
Qin, X., Wan, Y., Fan, M., Liao, Y., Li, Y., Wang, B., Gao, Q., Wu, H., Chen, X., 2020. Multiple stable isotopic signatures corroborate the predominance of acetoclastic methanogenesis during CH_4 formation in agricultural river networks. Agric. Ecosyst. Environ. 296, 106930 https://doi.org/10.1016/j.agee.2020.106930.
Queiroz, H.M., Artur, A.G., Taniguchi, C.A.K., da Silveira, M.R.S., do Nascimento, J.C., Nóbrega, G.N., Otero, X.L., Ferreira, T.O., 2019. Hidden contribution of shrimp farming effluents to greenhouse gas emissions from mangrove soils. Estuar. Coast. Shelf Sci. 221, 8–14. https://doi.org/10.1016/j.ecss.2019.03.011.
R Core Team, 2013. The R project for statistical computing. In: R Foundation for Statistical Computing. https://doi.org/10.9774/GLEAF.978-1-909493-38-4_2. Vienna, Austria.
Rawoof, S.A.A., Kumar, P.S., Vo, D.V., Subramanian, S., 2020. Sequential production of hydrogen and methane by anaerobic digestion of organic wastes: a review. Environ. Chem. Lett. 19, 1043–1063. https://doi.org/10.1007/s10311-020-01122-6.
Rosseel, Y., 2012. Lavaan: an R package for structural equation modeling. J. Stat. Softw. 48, 1–36. https://doi.org/10.18637/jss.v048.i02.
Rotaru, A.E., Thamdrup, B., 2016. A new diet for methane oxidizers. Science 351 (6274), 658. https://doi.org/10.1126/science.aaf0741.
Sabu, E.A., Gonsalves, M.J., Nazareth, D., Sreepada, R.A., 2022. Influence of environmental variables on methane related microbial activities in a tropical bio-secured zero-exchange shrimp culture system. Aquac. Rep. 100950 https://doi.org/10.1016/j.aqrep.2021.100950.
Sakai, S., Imachi, H., Hanada, S., Ohashi, A., Harada, H., Kamagata, Y., 2008. *Methanocella paludicola* gen. nov., sp. nov., a methane-producing archaeon, the first isolate of the lineage 'Rice cluster I', and proposal of the new archaeal order *Methanocellales* ord. nov. Int. J. Syst. Evol. Microbiol. 58 (4), 929–936. https://doi.org/10.1099/ijs.0.65571-0.
Saunois, M., Stavert, A.R., Poulter, B., Bousquet, P., Canadell, J.G., Jackson, R.B., Raymond, P.A., Dlugokencky, J.E., Houweling, S., Patra, P.K., Ciais, P., Arora, V.K., Bastviken, D., Bergamaschi, P., Blake, D.R., Brailsford, G., Bruhwiler, L., Carlson, K. M., Carrol, M., Castaldi, S., Chandra, N., Crevoisier, C., Crill, P.M., Covey, K., Curry, C.L., Etiope, G., Frankenberg, C., Gedney, N., Hegglin, M.I., Höglund-Isaksson, L., Hugelius, G., Ishizawa, M., Ito, A., Janssens-Maenhout, G., Jensen, K.M., Joos, F., Kleinen, T., Krummel, P.B., Langenfelds, R.L., Laruelle, G.G., Liu, L., Machida, T., Maksyutov, S., McDonald, K.C., McNorton, J., Miller, P.A., Melton, J.R., Morino, I., Müller, J., Murguia-Flores, F., Naik, V., Niwa, Y., Noce, S., O'Doherty, S., Parker, R.J., Peng, C., Peng, S., Peters, G.P., Prigent, C., Prinn, R., Ramonet, M., Regnier, P., Riley, W.J., Rosentreter, J.A., Segers, A., Simpson, I.J., Shi, H., Smith, S. J., Steele, L.P., Thornton, B.F., Tian, H., Tohjima, Y., Tubiello, F.N., Tsuruta, A., Viovy, N., Voulgarakis, A., Weber, T.S., Weele, M.V., Werf, G.R.V.D., Weiss, R.F., Worthy, D., Wunch, D., Yin, Y., Yoshida, Y., Zhang, W., Zhang, Z., Zhao, Y., Zheng, B., Zhu, Q., Zhu, Q., Zhuang, Q., 2020. The global methane budget 2000–2017. Earth Syst. Sci. Data 12, 1561–1623. https://doi.org/10.5194/essd-12-1561-2020.
Song, H., Liu, X., 2015. Anthropogenic effects on fluxes of ecosystem respiration and methane in the Yellow River estuary, China. Wetlands 36 (1), 113–123. https://doi.org/10.1007/s13157-014-0587-1.
Soto, J.O., 2021. Feed intake improvement, gut microbiota modulation and pathogens control by using Bacillus species in shrimp aquaculture. World J. Microbiol. Biotechnol. 37 (2), 1–7. https://doi.org/10.1007/s11274-020-02987-z.
Steinberg, L.M., Regan, J.M., 2008. Phylogenetic comparison of the methanogenic communities from an acidic, oligotrophic fen and an anaerobic digester treating municipal wastewater sludge. Appl. Environ. Microbiol. 74 (21), 6663–6671. https://doi.org/10.1128/AEM.00553-08.
Suárez-Abelenda, M., Ferreira, T.O., Camps-Arbestain, M., Rivera-Monroy, V.H., Macías, F., Nóbrega, G.N., Otero, X.L., 2014. The effect of nutrient-rich effluents from shrimp farming on mangrove soil carbon storage and geochemistry under semi-arid climate conditions in northern Brazil. Geoderma 213, 551–559. https://doi.org/10.1016/j.geoderma.2013.08.007.
Suhr, K.I., Letelier-Gordo, C.O., Lund, I., 2015. Anaerobic digestion of solid waste in RAS: effect of reactor type on the biochemical acidogenic potential (BAP) and assessment of the biochemical methane potential (BMP) by a batch assay. Aquac. Eng. 65–71 https://doi.org/10.1016/j.aquaeng.2014.12.005.

Tho, N., Ut, V.N., Merckx, R., 2011. Physico-chemical characteristics of the improved extensive shrimp farming system in the Mekong Delta of Vietnam. Aquac. Res. 42 (11), 1600–1614. https://doi.org/10.1111/j.1365-2109.2010.02750.x.

Tong, C., Cadillo-Quiroz, H., Zeng, Z.H., She, C.X., Yang, P., Huang, J.F., 2017. Changes of community structure and abundance of methanogens in soils along a freshwater–brackish water gradient in subtropical estuarine marshes. Geoderma 299, 101–110. https://doi.org/10.1016/j.geoderma.2017.03.026.

Tong, C., Bastviken, D., Tang, K.W., Yang, P., Yang, H., Zhang, Y., Guo, Q., Lai, D.Y.F., 2021. Annual CO_2 and CH_4 fluxes in coastal earthen ponds with *Litopenaeus vannamei* in southeastern China. Aquaculture 545, 737229. https://doi.org/10.1016/j.aquaculture.2021.737229.

Tully, K., Gedan, K., Epanchin-Niell, R., Strong, A., Bernhardt, E.S., BenDor, T., Mitchell, M., Kominoski, J., Jordan, T.E., Neubauer, S.C., Weston, N.B., 2019. The invisible flood: the chemistry, ecology, and social implications of coastal saltwater intrusion. Bioscience 69 (5), 368–378. https://doi.org/10.1093/biosci/biz027.

Waite, R., Beveridge, M., Brummett, R., Castine, S., Chaiyawannakarn, N., Kaushik, S., Mungkung, R., Nawapakpilai, S., Phillips, M., 2014. Improving productivity and environmental performance of aquaculture. WorldFish 1–59.

Wang, S., Giller, K., Kreuzer, M., Ulbrich, S.E., Braun, U., Schwarm, A., 2017. Contribution of ruminal fungi, archaea, protozoa, and bacteria to the methane suppression caused by oilseed supplemented diets. Front. Microbiol. 8, 1864. https://doi.org/10.3389/fmicb.2017.01864.

Wang, D., Song, C., Zhang, B., Chen, J., Luo, Wang, X., Wu, S., Ye, Y., 2021. Deciphering dissolved organic matter from freshwater aquaculture ponds in eastern China based on optical and molecular signatures. Process. Saf. Environ. Prot. 155, 122–130. https://doi.org/10.1016/j.psep.2021.09.025.

Wei, L., Ge, T., Zhu, Z., Ye, R., Peñuelas, J., Li, Y., Lynn, T.M., Jones, D.L., Wu, J., Kuzyakov, Y., 2022. Paddy soils have a much higher microbial biomass content than upland soils: a review of the origin, mechanisms, and drivers. Agric. Ecosyst. Environ. 326, 107798 https://doi.org/10.1016/j.agee.2021.107798.

Whiticar, M.J., 1999. Carbon and hydrogen isotope systematics of bacterial formation and oxidation of methane. Chem. Geol. 161 (1–3), 291–314. https://doi.org/10.1016/S0009-2541(99)00092-3.

Wilms, R., Sass, H., Köpke, B., Cypionka, H., Engelen, B., 2007. Methane and sulfate profiles within the subsurface of a tidal flat are reflected by the distribution of sulfate-reducing bacteria and methanogenic archaea. FEMS Microbiol. Ecol. 59, 611–621. https://doi.org/10.1111/j.1574-6941.2006.00225.x.

Wu, Y., Song, K., 2021. Anaerobic co-digestion of waste activated sludge and fish waste: methane production performance and mechanism analysis. J. Clean. Prod. 279, 123678 https://doi.org/10.1016/j.jclepro.2020.123678.

Xiao, L., Liu, F., Xu, H., Feng, D., Liu, J., Han, G., 2019. Biochar promotes methane production at high acetate concentrations in anaerobic soils. Environ. Chem. Lett. 17 (3), 347–1352. https://doi.org/10.1007/s10311-021-01251-6.

Xiao, L., Liu, F., Lichtfouse, E., Zhang, P., Li, F., 2020a. Methane production by acetate dismutation stimulated by *Shewanella oneidensis* and carbon materials: an alternative to classical CO_2 reduction. Chem. Eng. J. 389, 124469 https://doi.org/10.1016/j.cej.2020.124469.

Xiao, L., Zheng, S., Lichtfouse, E., Luo, M., Tan, Y., Liu, F., 2020b. Carbon nanotubes accelerate acetoclastic methanogenesis: from pure culture to anaerobic soil. Soil Biol. Biochem. 107938 https://doi.org/10.1016/j.soilbio.2020.107938.

Yang, P., Zhang, Y., Hong, Y., Zhang, Y., Xu, J., Tan, L., Tong, C., Lai Derrick, Y.F., 2019. Large Fine-Scale Spatiotemporal Variations of CH_4 Diffusive Fluxes From Shrimp Aquaculture Ponds Affected by Organic Matter Supply and Aeration in Southeast China. J. Geophys. Res. Biogeosci 124 (5), 1290–1307. https://doi.org/10.1029/2019JG005025.

Yang, P., Zhang, Y., Lai, D.Y.F., Tan, L., Jin, B., Tong, C., 2018. Fluxes of carbon dioxide and methane across the water-atmosphere interface of aquaculture shrimp ponds in two subtropical estuaries: the effect of temperature, substrate, salinity and nitrate. Sci. Total Environ. 635, 1025–1035. https://doi.org/10.1016/j.scitotenv.2018.04.102.

Yang, P., Zhang, Y., Yang, H., Guo, Q., Lai, D.Y., Zhao, G., Li, L., Tong, C., 2020. Ebullition was a major pathway of methane emissions from the aquaculture ponds in Southeast China. Water Res. 184, 116176. https://doi.org/10.1016/j.watres.2020.116176.

Ye, R., Jin, Q., Bohannan, B., Keller, J.K., McAllister, S.A., Bridgham, S.D., 2012. pH controls over anaerobic carbon mineralization, the efficiency of methane production, and methanogenic pathways in peatlands across an ombrotrophic–minerotrophic gradient. Soil Biol. Biochem. 54, 36–47. https://doi.org/10.1016/j.soilbio.2012.05.015.

Yuan, J., Xiang, J., Liu, D., Kang, H., He, T., Kim, S., Lin, Y., Freeman, C., Ding, W., 2019. Rapid growth in greenhouse gas emissions from the adoption of industrial-scale aquaculture. Nat. Clim. Chang. 9 (4), 318–322. https://doi.org/10.1038/s41558-019-0425-9.

Zhang, L., Wang, L., Yin, K., Lü, Y., Yang, Y., Huang, X., 2014. Spatial and seasonal variations of nutrients in sediment profiles and their sediment-water fluxes in the Pearl River estuary, Southern China. J. Earth Sci. 25 (1), 197–206. https://doi.org/10.1007/s12583-014-0413-y.

Zhang, Y., Qin, Z., Li, T., Zhu, X., 2022. Carbon dioxide uptake overrides methane emission at the air-water interface of algae-shellfish mariculture ponds: evidence from eddy covariance observations. Sci. Total Environ. 152867 https://doi.org/10.1016/j.scitotenv.2021.152867.

Zwietering, M.H., Jongenburger, I., Rombouts, F.M., Rief, K.V.T., 1990. Modeling of the bacterial growth curve. Appl. Environ. Microbiol. 56 (6), 1875–1881. https://doi.org/10.1128/AEM.56.6.1875-1881.1990.

Supplementary material

Aquaculture drastically increases methane production by favoring acetoclastic rather than hydrogenotrophic methanogenesis in shrimp pond sediments

Ji Tan[1,2,3,4], Eric Lichtfouse[5], Min Luo[2,4*], Yuxiu Liu[1,2,3], Fengfeng Tan[1,2,3], Changwei Zhang[1,2,4], Xin Chen[1,2,4], Jiafang Huang[1,2,3], Leilei Xiao[6**]

1 Key Laboratory of Humid Subtropical Eco-Geographical Process, Ministry of Education, Fujian Normal University, Fuzhou 350007, China; 2 Research Center of Geography and Ecological Environment, Fuzhou University, Fuzhou 350116, China; 3 College of Geography science, Fujian Normal University, Fuzhou 35008, China; 4 College of Environment and Safety Engineering, Fuzhou University, Fuzhou 350116, China; 5 Aix-Marseille Univ, CNRS, IRD, INRAE, CEREGE, Avenue Louis Philibert, Aixen Provence 13100, France; 6 CAS Key Laboratory of Coastal Environmental Processes and Ecological Remediation, Yantai Institute of Coastal Zone Research, Chinese Academy of Sciences, Yantai 264003, China.

*Corresponding authors: Min Luo, College of Environment and Safety Engineering, Fuzhou University, Wulongjiang North Avenue Street #2, Minhou County, Fuzhou 350116, China. E-mail: luomin@fzu.edu.cn. Leilei Xiao, CAS Key Laboratory of Coastal Environmental Processes and Ecological Remediation, Yantai Institute of Coastal Zone Research, Chinese Academy of Sciences, Yantai 264003, China. E-mail: llxiao@yic.ac.cn

Table S1 CO_2 and CH_4 production parameters (means ± standard deviation; n = 3) based on the modified Gompertz model (Zwietering et al., 1990) of the freshwater and oligohaline ponds in the Min River Estuary, southeast China.

Stages	Ponds	Incubation	M(t) ($\mu g \cdot g^{-1}$)	λ (d)	R_{max} ($\mu g \cdot g^{-1} \cdot d^{-1}$)	RMSE ($\mu g \cdot g^{-1}$)	*p*	R^2
CH_4 production								
Pre-farming	Freshwater	Control	2.78±0.12	0.00±0.00	0.16±0.02	0.23±0.02	<0.001	0.95
		With CH_3F	2.13±0.01	0.00±0.00	0.13±0.01	0.22±0.03	<0.001	0.93
	Oligohaline	Control	1.98±0.31	0.04±0.05	0.11±0.01	0.23±0.05	<0.001	0.98
		With CH_3F	1.56±0.29	1.68±0.80	0.08±0.01	0.24±0.07	<0.001	0.91
Farming	Freshwater	Control	13.58±3.10	0.04±0.06	0.54±0.06	1.07±0.07	<0.001	0.94
		With CH_3F	7.66±3.07	0.01±0.06	0.29±0.04	0.71±0.22	<0.001	0.91
	Oligohaline	Control	10.26±0.35	1.68±0.80	0.39±0.06	1.06±0.13	<0.001	0.98
		With CH_3F	5.47±0.82	0.20±0.34	0.39±0.03	0.58±0.17	<0.001	0.97
Post-farming	Freshwater	Control	12.71±1.83	0.07±0.07	0.44±0.03	0.74±0.13	<0.001	0.96
		With CH_3F	8.22±0.60	0.00±0.00	0.25±0.03	1.08±0.33	<0.001	0.94
	Oligohaline	Control	9.02±1.09	1.83±1.62	0.30±0.03	0.66±0.49	<0.001	0.98
		With CH_3F	4.66±0.78	1.63±1.55	0.17±0.02	0.72±0.21	<0.001	0.94
CO_2 production								
Pre-farming	Freshwater	Control	125.8±9.7	0.00±0.00	6.2±0.5	108.4±8.2	<0.001	0.85
		With CH_3F	125.7±11.4	0.00±0.00	9.3±0.9	110.1±9.9	<0.001	0.89
	Oligohaline	Control	150.0±16.8	0.00±0.00	8.2±1.1	120.3±18.4	<0.001	0.87
		With CH_3F	164.0±19.7	0.00±0.00	7.3±1.2	128.1±14.2	<0.001	0.86
Farming	Freshwater	Control	525.3±104.4	0.00±0.00	22.6±2.5	430.8±72.2	<0.001	0.91
		With CH_3F	507.1±119.6	0.00±0.00	25.8±2.6	422.6±90.4	<0.001	0.92
	Oligohaline	Control	570.4±144.5	0.00±0.00	29.5±3.9	474.0±111.0	<0.001	0.92
		With CH_3F	600.7±92.9	0.00±0.00	29.0±8.5	496.7±88.0	<0.001	0.90
Post-farming	Freshwater	Control	391.3±58.8	0.00±0.00	15.2±1.7	314.1±44.1	<0.001	0.87
		With CH_3F	410.5±43.7	0.00±0.00	16.2±3.7	325.1±43.8	<0.001	0.92
	Oligohaline	Control	366.8±53.0	0.00±0.00	17.8±1.0	305.4±38.0	<0.001	0.98
		With CH_3F	357.7±17.6	0.00±0.00	17.6±2.5	293.7±23.3	<0.001	0.95

M_t ($\mu g \cdot g^{-1}$): the cumulative methane production per gram of dry sediment; R_{max} ($\mu g \cdot g^{-1} \cdot d^{-1}$): the maximum methane production rates per gram of dry sediment; λ (d): time lag; RMSE ($\mu g \cdot g^{-1}$): root mean square error.

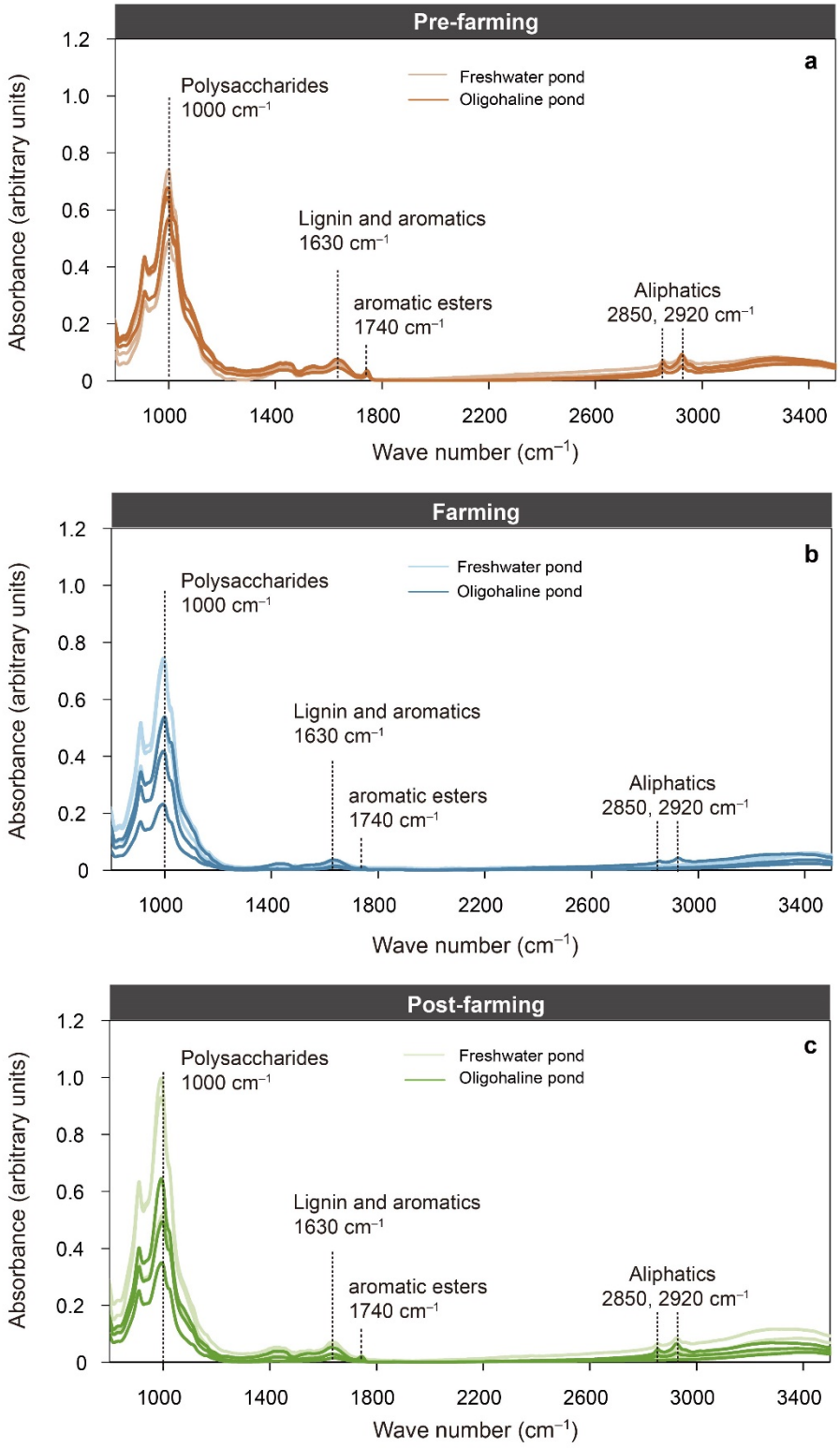

Figure S1 Fourier transform infrared (FTIR) spectroscopy within the region of 800 to 3500 cm^{-1} of the sediments of the freshwater and oligohaline ponds in the Min River Estuary, southeast China. References for wavenumbers according to Artz et al. (2007) and Parikh et al. (2014).

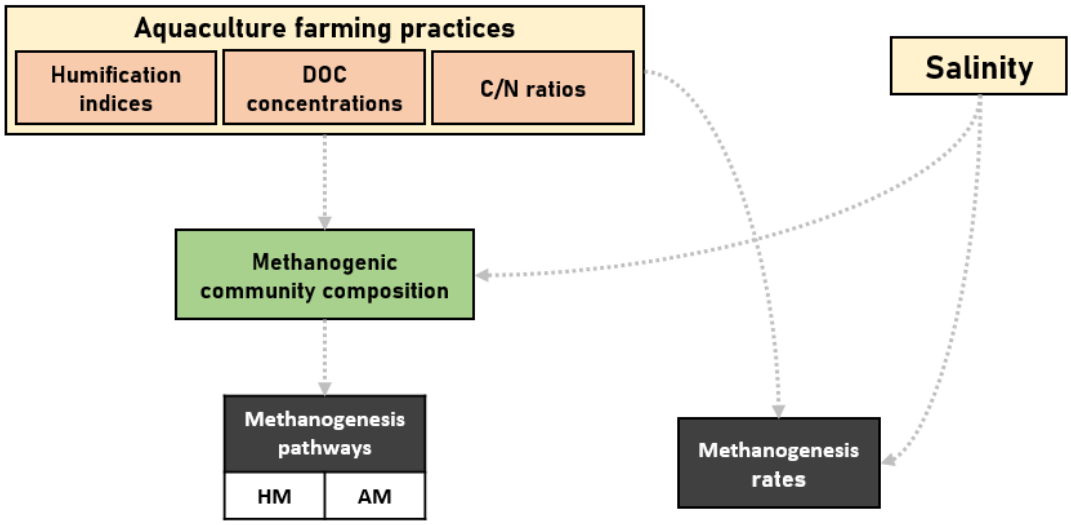

Figure S2 Hypothesized path model structure to evaluate the effects of aquaculture farming practices and salinity on rates and pathways of methanogenesis. DOC: dissolved organic carbon; HM: hydrogenotrophic methanogenesis; AM: acetoclastic methanogenesis.

Reference

Artz, R.R., Chapman, S.J., Robertson, A.J., Potts, J.M., Laggoun-Défarge, F., Gogo, S., Comont, L., Disnar J.R., Francez, A.J., 2008. FTIR spectroscopy can be used as a screening tool for organic matter quality in regenerating cutover peatlands. Soil Biol. Biochem. 40 (2), 515–527. https://doi.org/10.1016/j.soilbio.2007.09.019.

Parikh, S.J., Mukome, F., Zhang, X., 2014. Atr-ftir spectroscopic evidence for biomolecular phosphorus and carboxyl groups facilitating bacterial adhesion to iron oxides. Colloids Surf., B 119, 38–46. https://doi.org/10.1016/j.colsurfb.2014.04.022.

Zwietering, M.H., Jongenburger, I., Rombouts, F.M., Rief, K.V.T., 1990. Modeling of the Bacterial Growth Curve. Appl. Environ. Microbiol. 56 (6), 1875–1881. https://doi.org/10.1128/AEM.56.6.1875-1881.1990.